

### **Copyright Statement**

The author hereby certifies that the use of any copyrighted material in the thesis manuscript entitled: "Evaluation of NF-κB signaling in T cells" is appropriately acknowledged and, beyond brief excerpts, is with the permission of the copyright owner.

*Lara Kingeter*

Lara M. Kingeter

Emerging Infectious Diseases graduate program

Uniformed Services University of the Health Sciences

Report Documentation Page			Form Approved OMB No. 0704-0188	
<p>Public reporting burden for the collection of information is estimated to average 1 hour per response, including the time for reviewing instructions, searching existing data sources, gathering and maintaining the data needed, and completing and reviewing the collection of information. Send comments regarding this burden estimate or any other aspect of this collection of information, including suggestions for reducing this burden, to Washington Headquarters Services, Directorate for Information Operations and Reports, 1215 Jefferson Davis Highway, Suite 1204, Arlington VA 22202-4302. Respondents should be aware that notwithstanding any other provision of law, no person shall be subject to a penalty for failing to comply with a collection of information if it does not display a currently valid OMB control number.</p>				
1. REPORT DATE <b>2009</b>	2. REPORT TYPE	3. DATES COVERED <b>00-00-2009 to 00-00-2009</b>		
4. TITLE AND SUBTITLE <b>Evaluation Of NF-&amp;#954;B Signaling In T cells</b>		5a. CONTRACT NUMBER		
		5b. GRANT NUMBER		
		5c. PROGRAM ELEMENT NUMBER		
6. AUTHOR(S)		5d. PROJECT NUMBER		
		5e. TASK NUMBER		
		5f. WORK UNIT NUMBER		
7. PERFORMING ORGANIZATION NAME(S) AND ADDRESS(ES) <b>Uniformed Services University of the Health Sciences,4301 Jones Bridge Rd,Bethesda,MD,20814</b>		8. PERFORMING ORGANIZATION REPORT NUMBER		
9. SPONSORING/MONITORING AGENCY NAME(S) AND ADDRESS(ES)		10. SPONSOR/MONITOR'S ACRONYM(S)		
		11. SPONSOR/MONITOR'S REPORT NUMBER(S)		
12. DISTRIBUTION/AVAILABILITY STATEMENT <b>Approved for public release; distribution unlimited</b>				
13. SUPPLEMENTARY NOTES				
14. ABSTRACT <b>T cell activation of the transcription factor NF-&amp;#954;B is a tightly controlled process and many of the proteins involved in this signal transduction pathway have been identified. The proteins PKC&amp;#952;, Bcl10, and Malt1 are known to play a role in the T cell receptor (TCR) mediated activation of NF-&amp;#954;B, but the precise role of these proteins has not been characterized. To better understand the function of PKC&amp;#952;, Bcl10, and Malt1 in this pathway, we examined NF-&amp;#954;B activation in T cells deficient in these proteins. Our results show that the loss of PKC&amp;#952;, Bcl10, or Malt1 differentially affects CD4+ and CD8+ T cells. Knock-out CD4+ T cells showed a severe defect in proliferation, upregulation of activation markers, and phosphorylation of I&amp;#954;B&amp;#945; (a surrogate marker of NF-&amp;#954;B activation) in response to TCR ligation. In contrast, CD8+ T cells were only slightly impaired in proliferation and I&amp;#954;B&amp;#945; phosphorylation, and showed nearly normal upregulation of activation markers, especially in response to strong TCR stimulus. Taken together, these data indicate differences in the way mature CD4+ and CD8+ T cells signal to NF-&amp;#954;B, and suggest that in the absence of PKC&amp;#952;, Bcl10, or Malt1, CD8+ T cells utilize a parallel pathway to activate NF-&amp;#954;B under conditions of strong TCR stimulation.</b>				
15. SUBJECT TERMS				
16. SECURITY CLASSIFICATION OF:			17. LIMITATION OF ABSTRACT <b>Same as Report (SAR)</b>	18. NUMBER OF PAGES <b>71</b>
a. REPORT <b>unclassified</b>	b. ABSTRACT <b>unclassified</b>	c. THIS PAGE <b>unclassified</b>	19a. NAME OF RESPONSIBLE PERSON	

## **Abstract**

T cell activation of the transcription factor NF- $\kappa$ B is a tightly controlled process, and many of the proteins involved in this signal transduction pathway have been identified. The proteins PKC $\theta$ , Bcl10, and Malt1 are known to play a role in the T cell receptor (TCR) mediated activation of NF- $\kappa$ B, but the precise role of these proteins has not been characterized. To better understand the function of PKC $\theta$ , Bcl10, and Malt1 in this pathway, we examined NF- $\kappa$ B activation in T cells deficient in these proteins. Our results show that the loss of PKC $\theta$ , Bcl10, or Malt1 differentially affects CD4 $^{+}$  and CD8 $^{+}$  T cells. Knock-out CD4 $^{+}$  T cells showed a severe defect in proliferation, upregulation of activation markers, and phosphorylation of I $\kappa$ B $\alpha$  (a surrogate marker of NF- $\kappa$ B activation) in response to TCR ligation. In contrast, CD8 $^{+}$  T cells were only slightly impaired in proliferation and I $\kappa$ B $\alpha$  phosphorylation, and showed nearly normal upregulation of activation markers, especially in response to strong TCR stimulus. Taken together, these data indicate differences in the way mature CD4 $^{+}$  and CD8 $^{+}$  T cells signal to NF- $\kappa$ B, and suggest that in the absence of PKC $\theta$ , Bcl10, or Malt1, CD8 $^{+}$  T cells utilize a parallel pathway to activate NF- $\kappa$ B under conditions of strong TCR stimulation.

Given the importance of NF- $\kappa$ B in T cell biology and function, we sought to characterize the digital or analog nature of TCR-mediated NF- $\kappa$ B activation. We found that I $\kappa$ B $\alpha$  and p65 phosphorylation occurs in a digital fashion, with the intensity of the phosphorylation response independent of the intensity of TCR stimulation. We propose and discuss two independent models to account for these results.

**Evaluation of NF-κB signaling in T cells**

**By**

**Lara M. Kingeter**

**Dissertation submitted to the Faculty of the Emerging Infectious Diseases program,**

**Uniformed Services University of the Health Sciences**

**In partial fulfillment of the requirements for the degree of**

**Doctor of Philosophy, 2009**

## **Acknowledgments**

Many thanks to my advisor, Dr. Brian Schaefer, for his guidance, encouragement, support, and patience through the years.

Thanks to my thesis committee members, Drs. Davies, Dveksler, Merrell, Schaefer, and Snapper for your suggestions and contributions to these projects.

Thanks to the members of the Schaefer lab, past and present, for all the help (especially Sean, the best mouse tech ever!).

Thanks to Brett, Christine, Felicia, Stephanie, Rachel, Jess, Ellen, Eric, Kristy, Rob, Doug, Sean, John, Katie, Katherine, Sam, Randall, JR, Tammy, James, Hossein, Ryan, Krystle, Tom, Julie, Kenny, Tara, and Alisa for all the great memories!

Finally, thanks to my family – Mom, Dad, Adam, and Jacq – for all of the love and support.

## Table of Contents

Approval Page.....	i
Copyright Statement.....	ii
Abstract.....	iii
Title Page.....	iv
Acknowledgments.....	v
Table of Contents.....	vi
Table of Tables.....	ix
Table of Figures.....	x
Chapter 1: Introduction .....	1
Introduction to T cells.....	1
T cells in the adaptive immune response .....	2
Introduction to T cell signaling.....	5
T cells and transcription factors.....	8
NFAT and AP-1: activation and function.....	8
NF-κB: an introduction.....	9
Canonical regulation of NF-κB signaling.....	9
Non-canonical activation of NF-κB.....	12
TCR signaling to NF-κB.....	14
The function of NF-κB .....	16

Introduction to thesis topics .....	17	
References.....	20	
Chapter 2: Loss of Protein Kinase C $\theta$ , Bcl10, or Malt1 Selectively Impairs Proliferation and NF- $\kappa$ B Activation in the CD4 $^{+}$ T Cell Subset. ....		24
Abstract and Introduction.....	25	
Materials and Methods.....	26	
Results.....	26	
Discussion.....	33	
Acknowledgments.....	34	
References.....	34	
Chapter 3: The terminal events in TCR-mediated activation of NF- $\kappa$ B are digital.....		36
Abstract.....	37	
Introduction.....	38	
Materials and Methods.....	41	
Results and Discussion.....	43	
References.....	50	
Chapter 4: Discussion.....		51
Review of Chapter 2 results.....	51	
CD4 $^{+}$ and CD8 $^{+}$ T cells display differential signaling.....	52	
A parallel pathway?.....	54	
What are the roles of PKC $\theta$ , Bcl10, and Malt1 in TCR signaling to NF- $\kappa$ B?.....	55	

Additional future studies.....	58
Review of Chapter 3 results.....	60
When does the signal become digital?.....	61
Potential role for the IKK complex.....	61
Non-traditional tools to explore signaling.....	63
Thesis summary.....	64
References.....	65
Appendix: Expanding the multicolor capabilities of basic confocal microscopes by employing red and near-infrared quantum dot conjugates.....	67
Abstract.....	68
Background.....	70
Results and Discussion.....	72
Conclusion.....	80
Methods.....	81
Authors' contributions.....	85
Acknowledgments.....	85
References.....	86

## **Table of Tables**

Table 1. Confocal microscope parameters.....	74
--	----

## Table of Figures

### Chapter 1: Introduction

Figure 1. Naïve T cell activation occurs in lymph nodes.....	3
Figure 2. The T cell receptor complex.....	5
Figure 3. Early TCR signaling events.....	7
Figure 4. Structure of NF-κB family members.....	9
Figure 5. Structure of IκB proteins.....	10
Figure 6. Proteins of the IKK complex.....	11
Figure 7. Various pathways lead to canonical NF-κB activation.....	12
Figure 8. Non-canonical NF-κB activation.....	13
Figure 9. TCR mediated activation of NF-κB.....	14
Figure 10. Structure of PKCθ, Carma1, Bcl10, and Malt1.....	15

### Chapter 2: Loss of Protein Kinase Cθ, Bcl10, or Malt1 Selectively Impairs Proliferation and NF-κB Activation in the CD4+ T Cell Subset

Figure 1. CD4 <sup>+</sup> T cells from PKCθ <sup>-/-</sup> , Bcl10 <sup>-/-</sup> , and Malt1 <sup>-/-</sup> mice fail to proliferate in response to TCR stimulation.....	27
Figure 2. Defects in PKCθ <sup>-/-</sup> CD4 <sup>+</sup> T cell proliferation in response to specific Ag stimulation.....	28
Figure 3. PKCθ <sup>-/-</sup> , Bcl10 <sup>-/-</sup> , and Malt1 <sup>-/-</sup> T cells show defects in IL-2 production, but up-regulate CD44 and CD25 after TCR ligation.....	28
Figure 4. IL-2 fails to rescue knockout CD4 <sup>+</sup> T cell proliferation.....	29
Figure 5. Ectopic IL-2 improves knockout CD8 <sup>+</sup> T cell survival.....	30
Figure 6. Differential IκBα phosphorylation in CD4 <sup>+</sup> and CD8 <sup>+</sup> T cells from PKCθ <sup>-/-</sup> , Bcl10 <sup>-/-</sup> , and Malt1 <sup>-/-</sup> mice.....	31

Figure 7. PKC $\theta^{-/-}$ T cells show defective p65 nuclear localization.....	32
Chapter 3: The terminal events in TCR-mediated activation of NF- $\kappa$ B are digital	
Figure 1. TCR-mediated phosphorylation of I $\kappa$ B $\alpha$ is digital.....	44
Figure 2. Digital I $\kappa$ B $\alpha$ phosphorylation in response to peptide antigen stimulation.....	46
Figure 3. p65 phosphorylation is digital.....	47
Figure 4. Two models of NF- $\kappa$ B signaling.....	48
Chapter 4: Discussion	
Figure 1. CD4 $^{+}$ and CD8 $^{+}$ T cells show differential reliance on PKC $\theta$ , Bcl10, and Malt1.....	54
Figure 2. Proposed model of signal digitization at the IKK complex.....	62
Appendix: Expanding the multicolor capabilities of basic confocal microscopes by employing red and near-infrared quantum dot conjugates.	
Figure 1. Filter configuration and data acquisition strategy for 6-parameter imaging experiments.....	74
Figure 2. Alexa 555 and Qdot 655 secondary antibodies produce images of similar quality.....	75
Figure 3. Qdot reagents expand the number of fluorophores detectable in a single experiment.....	78
Figure 4. Details of 3T3-APC/T cell interaction showing distribution of cellular proteins and structures.....	79



## **Chapter 1: Introduction**

The studies presented in this thesis describe experiments designed to increase our understanding of how T cells transduce activating signals to the transcription factor NF- $\kappa$ B, and to better understand the kinetic nature of NF- $\kappa$ B signaling. The overarching goals of this thesis are 1) to evaluate T cell receptor mediated activation of the transcription factor NF- $\kappa$ B in the absence of key signaling proteins, and 2) to define the mechanisms of signal transduction to NF- $\kappa$ B by identifying the point at which signaling becomes digital in nature.

### ***Introduction to T cells***

A T cell is a specialized type of lymphocyte. T cells are so named because these cells undergo developmental maturation in the thymus, an organ that sits above the heart (reviewed in (1)). All T cells express a T cell receptor (TCR); the composition of the TCR can be classified as either  $\alpha\beta$  or  $\gamma\delta$ , based on which types of receptor components are expressed.  $\alpha\beta$  T cells are perhaps the best understood, and will be the focus of this dissertation.

T cell development begins when thymocyte precursor cells migrate from the bone marrow to the thymus. Once in the thymus, precursor cells engage in a series of interactions with thymic stromal and epithelial cells. These interactions provide signals for developing T cells (thymocytes) that guide the maturation of the cell and the expression of various surface proteins. Thymocytes undergo at least 4 stages of maturation, characterized by their expression of a TCR and the co-receptors CD4 and

CD8. The final product of thymic maturation is a mature T cell expressing a TCR complex and a CD4 or CD8 co-receptor.

While T cells are developing in the thymus, they are exposed to selection processes that identify and destroy cells that would function inappropriately in the periphery. This selection process helps ensure T cell tolerance to self by weeding out those cells that recognize and are activated by self-antigen. During interactions with thymic stromal cells, thymocytes expressing a TCR that binds too strongly to self-antigens are induced to undergo apoptosis. Conversely, thymocytes that express a TCR that only weakly binds self-antigen die by neglect, as they cannot receive the necessary signals for maturation. The destruction of these cells ensures that only T cells capable of properly interacting with self-cells continue to develop. The surviving population of thymocytes express a TCR that allows them to interact with self-cells, while not becoming activated by self-antigen.

### ***T cells in the adaptive immune response***

T cells play a critical role in the adaptive immune response to pathogens. Naïve (i.e. antigen inexperienced) T cells continually circulate through the body via the circulatory and lymphatic systems. Naïve T cells enter lymph nodes or the spleen through lymphatic vessels; once there, T cells interact with dendritic cells and macrophages, two types of antigen presenting cell (Fig. 1). Under normal conditions, this interaction does not lead to the activation of the T cell, and the T cell returns to the circulation to travel to another lymph node. However, during an infection, dendritic cells and macrophages present pathogen derived antigen to the T cells. T cells that recognize

the foreign peptide undergo clonal expansion, successive rounds of proliferation that increase the number of T cells specific for the foreign antigen.

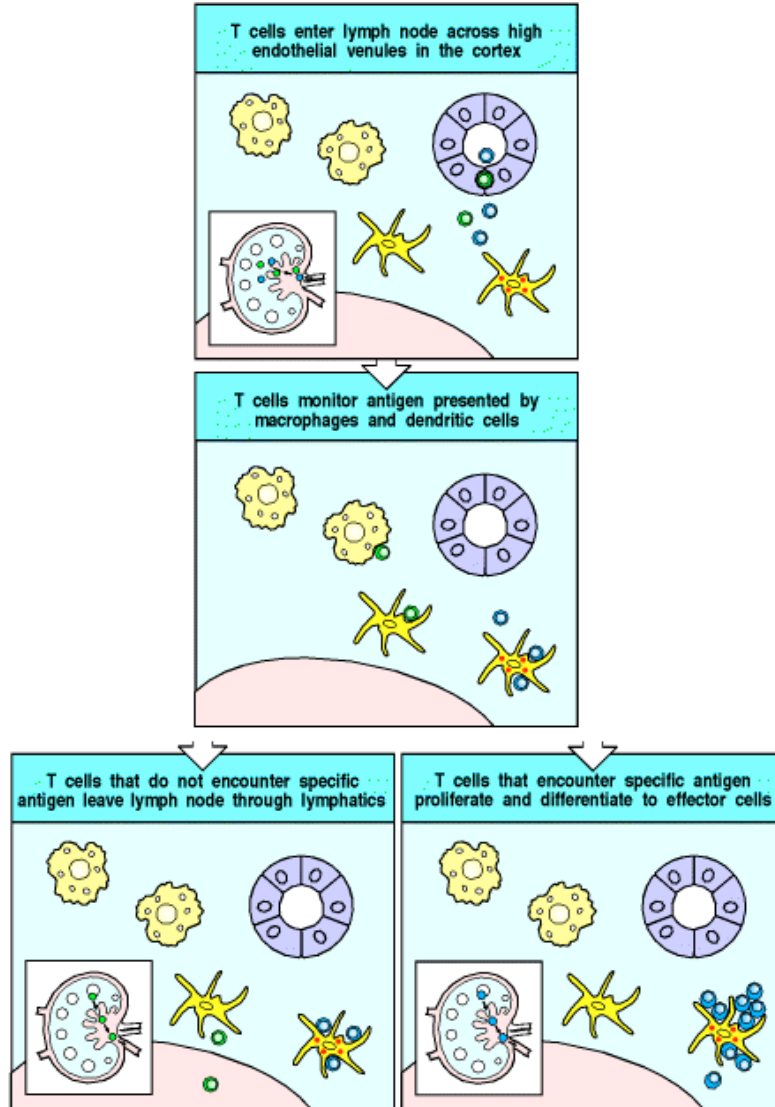


**Figure 1. Naïve T cell activation occurs in lymph nodes (adapted from (1)).** Naïve T cells enter lymph nodes from the circulation and interact with dendritic cells and macrophages. In an uninfected host, the T cell does not become activated and re-enters the circulation. During an infection, this interaction leads to T cell activation and clonal expansion.

During antigen encounter and clonal expansion T cells acquire effector functions which allow the T cell to provide help for B cells, secrete cytokines that influence the behavior of other cells such as macrophages and dendritic cells, and participate in the

killing of infected cells. CD4<sup>+</sup> T cells can be further classified into different types of effector cells, depending on their cytokine profile and functional responses. There are at least 4 major effector types identified thus far: T<sub>H</sub>1, T<sub>H</sub>2, T<sub>H</sub>17, and Treg. Each effector type produces a characteristic panel of cytokines: for example, T<sub>H</sub>1 cells produce IFN- $\gamma$ ; T<sub>H</sub>2 cells are characterized by IL-4 production; T<sub>H</sub>17 cells produce IL-17 and IL-21, and Treg cells produce the immunosuppressive cytokines IL-10 and TGF- $\beta$ . The combination of cytokines produced by different effector CD4<sup>+</sup> T cells directs the immune response to various classes of pathogen. As a simplified example, infection with a bacterial pathogen will trigger the differentiation of CD4<sup>+</sup> T cells into T<sub>H</sub>1 cells, while infection with a multicellular parasite will trigger the differentiation of T<sub>H</sub>2 cells.

Effector T cells migrate out of the lymph node and travel to the site of infection via chemotaxis. Once there, effector cells participate in the clearance of the pathogen by directing the behavior of other immune cells (CD4<sup>+</sup> T cells) or by directly killing infected cells (CD8<sup>+</sup> T cells). Because effector T cells are powerful mediators of the immune response, they are potentially dangerous to healthy tissue. For this reason, effector cells are short-lived, and die at the conclusion of an immune response by undergoing ‘activation induced cell death’. This process virtually eliminates the population of effector T cells, minimizing the potential damage to healthy tissue.

While effector T cells play a role in the acute immune response to a pathogen, there is an additional population of T cells that develops during an immune response. Memory T cells are a long-lived population of antigen-experienced cells that help provide immunological memory, the ability to rapidly respond to a previously encountered pathogen. Although the generation of memory T cells is not altogether understood

(reviewed in (2)), memory T cells circulate through the body and undergo rapid clonal expansion following secondary encounter with antigen, either in the lymph node or in the periphery.

### ***Introduction to T cell signaling***

As mentioned above, all mature T cells display a TCR. For  $\alpha\beta$  T cells, the TCR consists of an  $\alpha$  and  $\beta$  chain. During T cell development, the genes encoding the variable regions of the  $\alpha$  and  $\beta$  chains undergo a series of recombination events that result in the generation of unique  $\alpha$  and  $\beta$  chains (reviewed in (3, 1)). On a population level, these recombination events generate a staggering amount of receptor diversity, ensuring that the mature T cell population will be able to respond to a variety of pathogens.

As shown in Figure 2, the  $\alpha$  and  $\beta$  chains of the TCR form a complex with CD3, a surface protein with membrane-spanning and intracellular regions.

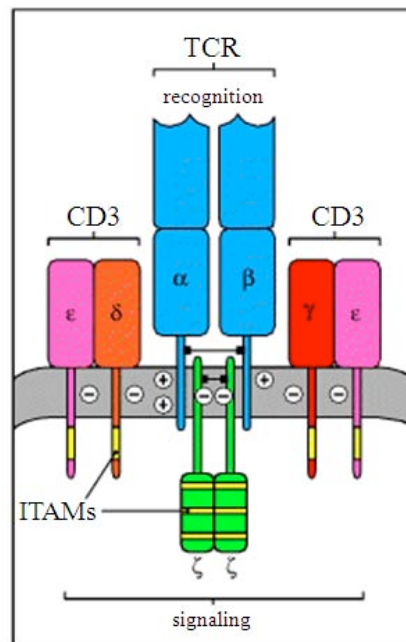


**Figure 2. The T cell receptor complex (1).** TCR  $\alpha$  and  $\beta$  chains form a complex with CD3 proteins. The resulting TCR complex contains intracellular domains important in signal transduction (ITAMs).

The intracellular regions of the TCR complex contain ITAM motifs (immunoreceptor tyrosine based activation motifs), which are important in signal transduction (reviewed in (4)). The resulting TCR receptor complex recognizes peptide antigens displayed in the context of a major histocompatibility complex (MHC) molecule on the surface of an antigen presenting cell (APC). There are 2 structural variants of MHC molecule: MHCI and MHCII. There are a variety of genes which encode MHC proteins, resulting in a diversity of MHC molecules capable of interacting with T cell receptors (reviewed in (1)). The type of MHC molecule with which a T cell can interact is dictated by the T cell expression of the co-receptor proteins, CD4 and CD8. CD4 and CD8 serve to stabilize the interaction between the TCR and MHC protein: CD4<sup>+</sup> T cells interact with MHCII molecules, while CD8<sup>+</sup> T cells interact with MHCI molecules (reviewed in (5)).

Regardless of the type of MHC interaction, when a TCR encounters its cognate peptide antigen a series of intracellular signal transduction events is initiated, which culminate in the activation of the T cell. A simplified schematic of early TCR signaling events is depicted in Figure 3.

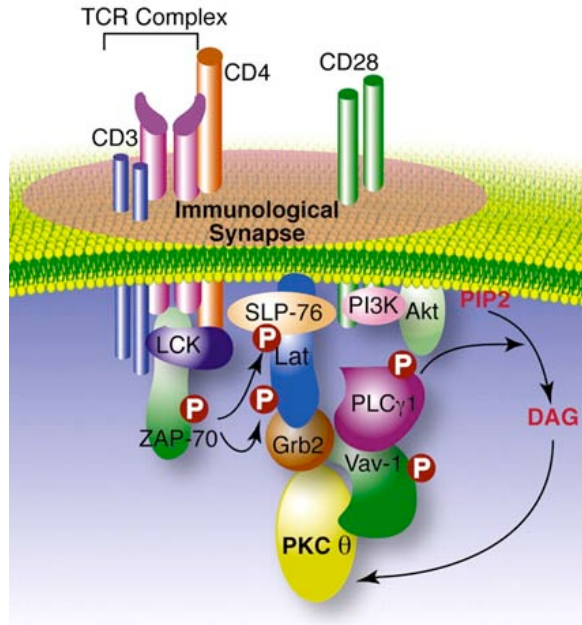


**Figure 3. Early TCR signaling events (6).** TCR ligation triggers early phosphorylation events that recruit adaptor proteins involved in various signal transduction cascades.

Almost immediately after a TCR encounters its cognate antigen, the Src family protein tyrosine kinase Lck phosphorylates the ITAMs of the TCR (7). Zap-70 (Zeta chain associated protein kinase of 70 kDa) is recruited to the phosphorylated ITAMs, and the association between Zap70 and the ITAM disrupts the inhibitory conformation of Zap70 (8), allowing Zap70 to be phosphorylated (and subsequently activated) by Lck (9). Activated Zap70 recruits and phosphorylates LAT (linker for activation of T cells) (10); activated LAT then associates with a variety of proteins, including phospholipase-C $\gamma$ 1 (PLC- $\gamma$ 1), the Grb2-SOS-Ras complex, and phosphatidylinositol 3-kinase (PI3K), (reviewed in (11)). Zap-70 also phosphorylates and activates SLP-76 (SH2-domain containing lymphocyte protein of 76 kDa); SLP-76 cooperates with LAT to activate PLC- $\gamma$ 1 and Grb2 (12). These proximal signaling events induce signal transduction cascades

which ultimately culminate in the activation of three key transcription factors, NFAT, AP-1, and NF-κB.

### ***T cells and transcription factors***

Transcription factors are proteins that control the transcriptional expression of target genes (reviewed in (1)). Transcription factors bind to DNA consensus sequences upstream of target genes; once bound, they can activate or repress the expression of genes, depending on whether they enhance or interfere with the recruitment of DNA dependent RNA polymerase. There are three major transcription factors involved in controlling T cell activation, proliferation, and gain of effector function: NFAT (nuclear factor of activated T cells), AP-1, and NF-κB (nuclear factor kappa b).

### ***NFAT and AP-1: activation and function***

The NFAT family consists of 5 proteins, 4 of which are regulated by calcium (NFAT signaling is extensively reviewed in (13, 14, 15)). Under resting conditions, NFAT is phosphorylated and remains in the cytoplasm. Following TCR ligation, activation of PLC-γ1 results in an increase in intracellular Ca<sup>2+</sup> levels through the release of endoplasmic reticulum Ca<sup>2+</sup> stores. This spike in intracellular calcium triggers a positive feedback mechanism, whereby membrane Ca<sup>2+</sup> channels open to allow for the influx of additional Ca<sup>2+</sup>. As cytoplasmic Ca<sup>2+</sup> levels increase, the phosphatase calcineurin becomes activated and dephosphorylates NFAT. NFAT is then able to enter the nucleus and bind to NFAT consensus sites to control transcription of target genes.

AP-1 is a heterodimer composed of Fos and Jun family members (reviewed in (16)). The components of AP-1 are not expressed in resting T cells, and are synthesized in response to TCR ligation and activation of the MAPK/Ras pathway (17). NFAT and

AP-1 can bind cooperatively to NFAT:AP-1 consensus sequences in gene promoter regions. Together, NFAT and AP-1 are involved in regulating the T cell expression of several cytokines, including IL-2, IL-4, GM-CSF, and TNF- $\alpha$  (13).

### ***NF- $\kappa$ B: an introduction***

A transcription factor of central importance, NF- $\kappa$ B was originally discovered in B cells, and was named due to its role in controlling the expression of the kappa light chain (18). NF- $\kappa$ B has since been found to be ubiquitously expressed in nucleated cells, and this transcription factor plays a major role in controlling cellular proliferation and apoptosis (reviewed extensively in (19, 20, 21)). For cells of the immune system, and T cells in particular, NF- $\kappa$ B activation is required for proliferation and gain of effector function.

### ***Canonical regulation of NF- $\kappa$ B signaling***

NF- $\kappa$ B is a family of 5 proteins that form homo or heterodimers (depicted in Figure 4).

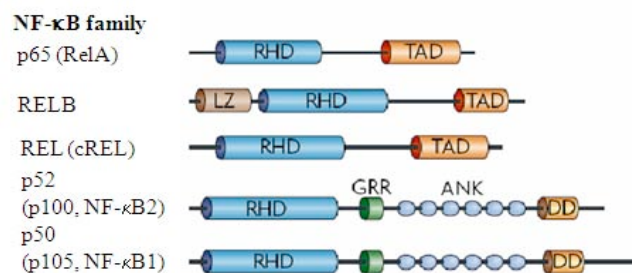


**Figure 4. Structure of NF- $\kappa$ B family members (21).** The 5 NF- $\kappa$ B proteins can homo or heterodimerize via interactions between Rel homology domains (RHD). TAD domains are responsible for DNA binding.

RelA, RelB, c-Rel, p100/p52, and p105/p50 share structural similarities, among them a Rel homology domain, which allows dimerization of the subunits and binding to

DNA, and a transcription activating domain (found only in p65, RelB, and cRel). The term ‘NF-κB’ traditionally refers to the RelA/p50 heterodimer.

Regardless of the cell type, the terminal canonical NF-κB activation steps are well conserved (reviewed in (19, 20, 21)). Under normal, resting conditions, NF-κB is retained in the cytoplasm through its association with IκB proteins (inhibitor of κB proteins). There are 6 identified IκB proteins, depicted in Figure 5.

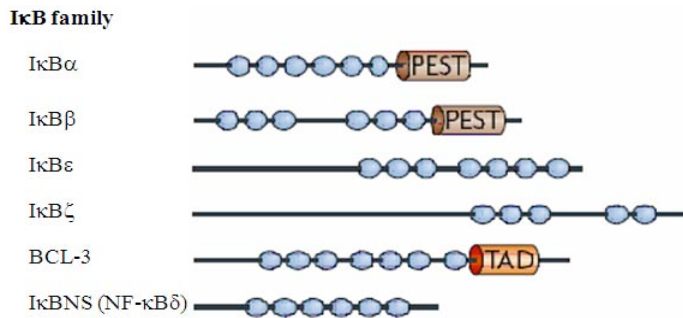


**Figure 5. Structure of IκB proteins (21).** IκB proteins bind to the NF-κB dimer and mask its nuclear localization sequence, keeping the complex in the cytoplasm.

The traditional IκB proteins (IκB $\alpha$ , IκB $\beta$ , IκB $\epsilon$  – Fig. 5) bind to the NF-κB dimer and mask its nuclear localization sequence, preventing the complex from entering the nucleus. Following a stimulatory event, the IKK complex (inhibitor of κB kinase complex) becomes activated. The IKK complex consists of 3 subunits: the kinase subunits IKK $\alpha$  and IKK $\beta$ , and the regulatory subunit IKK $\gamma$  (Fig. 6). IKK $\alpha$  is specifically activated during non-canonical (i.e. IKK $\alpha$ -mediated) signaling, while canonical signaling is mediated by IKK $\beta$ .

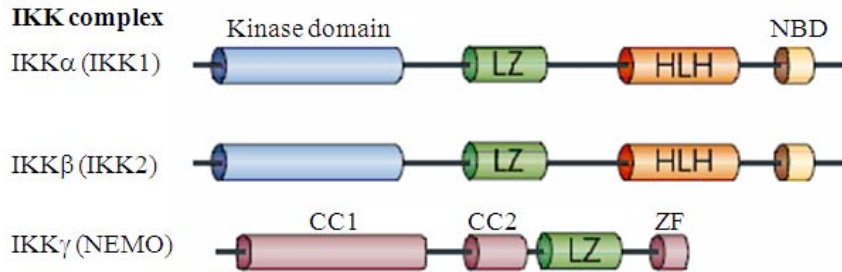


**Figure 6. Proteins of the IKK complex** (21). IKK $\alpha$  and IKK $\beta$  are kinases, while IKK $\gamma$  functions as a regulatory subunit. Abbreviations: LZ – leucine zipper; HLH – helix loop helix; NBD – nuclear binding domain; ZF – zinc finger; CC1 and CC2 – coiled coiled region 1 and 2, respectively.

After IKK activation, IKK $\beta$  phosphorylates I $\kappa$ B $\alpha$  on conserved serine residues (22, 23). This phosphorylation triggers poly-ubiquitination of I $\kappa$ B $\alpha$  on lysine residues (23), leading to its proteasomal degradation and freeing NF- $\kappa$ B to enter the nucleus and control the transcription of target genes. One of the genes controlled by NF- $\kappa$ B is that of I $\kappa$ B $\alpha$ ; therefore, one of the consequences of NF- $\kappa$ B activation is the synthesis of its own inhibitor (24, 25). Newly synthesized I $\kappa$ B $\alpha$  enters the nucleus and binds to NF- $\kappa$ B, shuttling it out of the nucleus and back into the cytoplasm.

Canonical NF- $\kappa$ B activation can be triggered by a variety of stimuli, including B and T cell receptor engagement, TNF receptor signaling, and IL-1R/Toll-like receptor signaling (Fig. 7).

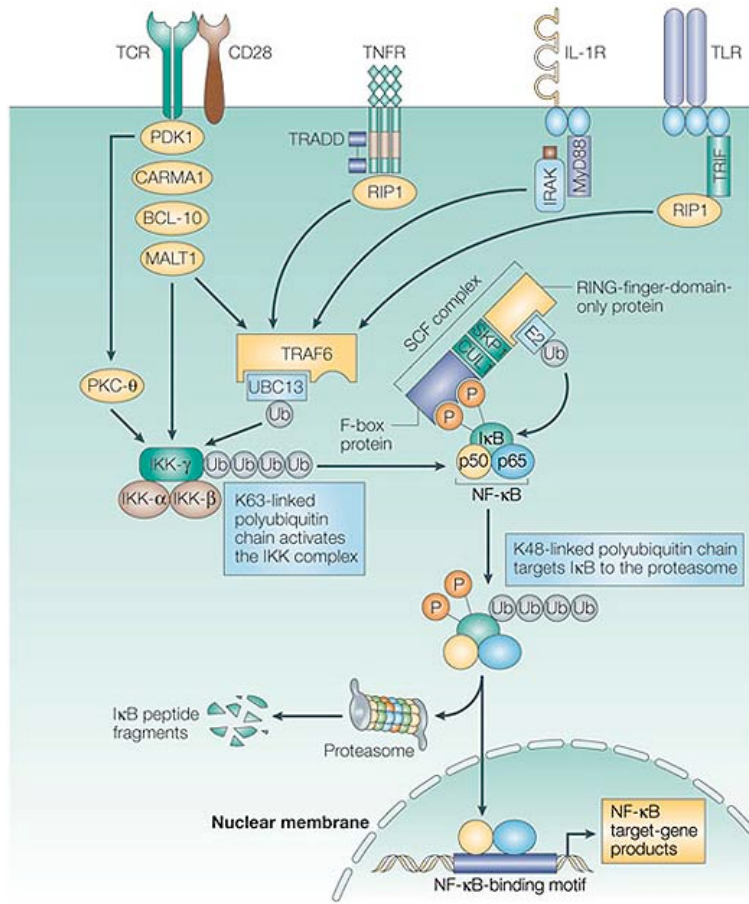


**Figure 7. Various pathways lead to canonical NF-κB activation (26).** TCR, TNFR, IL-1R, and TLR signaling all recruit specific adaptor proteins, which leads to the ubiquitination and activation of the IKK complex, resulting in IKK $\beta$  mediated phosphorylation and subsequent proteasomal destruction of I $\kappa$ B $\alpha$  and the release of NF-κB.

While the proximal signaling events for each pathway are distinct (reviewed in (27, 26)), the pathways converge at the ubiquitination and activation of the IKK complex, which triggers IKK $\beta$  mediated phosphorylation of I $\kappa$ B $\alpha$ , followed by ubiquitination and proteasomal degradation of this protein as described.

### ***Non-canonical activation of NF-κB***

In T cells, NF-κB can be activated via one of two general pathways. TCR triggered canonical (IKK $\beta$ -mediated) signaling is the focus of this thesis and will be

explained in greater detail, but the non-canonical (IKK $\alpha$ -mediated) pathway deserves a mention as well. A depiction of the non-canonical pathway can be found in Figure 8.

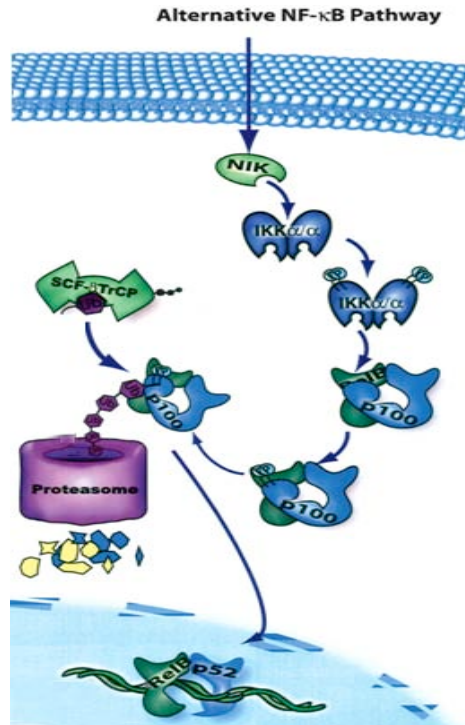


**Figure 8. Non-canonical NF-κB activation (19).** NIK activates IKK $\alpha$ , triggering the proteasomal processing of p100 to p52.

During non-canonical NF-κB activation, a stimulus such as lymphotoxin  $\beta$  signaling or CD40L binding triggers the activation of NIK (NF-κB inducing kinase) (reviewed in (28)). NIK in turn activates the IKK $\alpha$  subunit of the IKK complex (29). Activated IKK $\alpha$  phosphorylates p100; this phosphorylation event triggers the ubiquitination and subsequent proteasomal processing of p100 to p52. The resulting p52 protein is free to heterodimerize with other NF-κB family members such as RelB, and this dimer enters the nucleus to control transcription of target genes.

### TCR signaling to NF- $\kappa$ B

As previously mentioned, TCR signaling results in the canonical activation of NF- $\kappa$ B, and a simplified depiction of this pathway can be found in Figure 9.

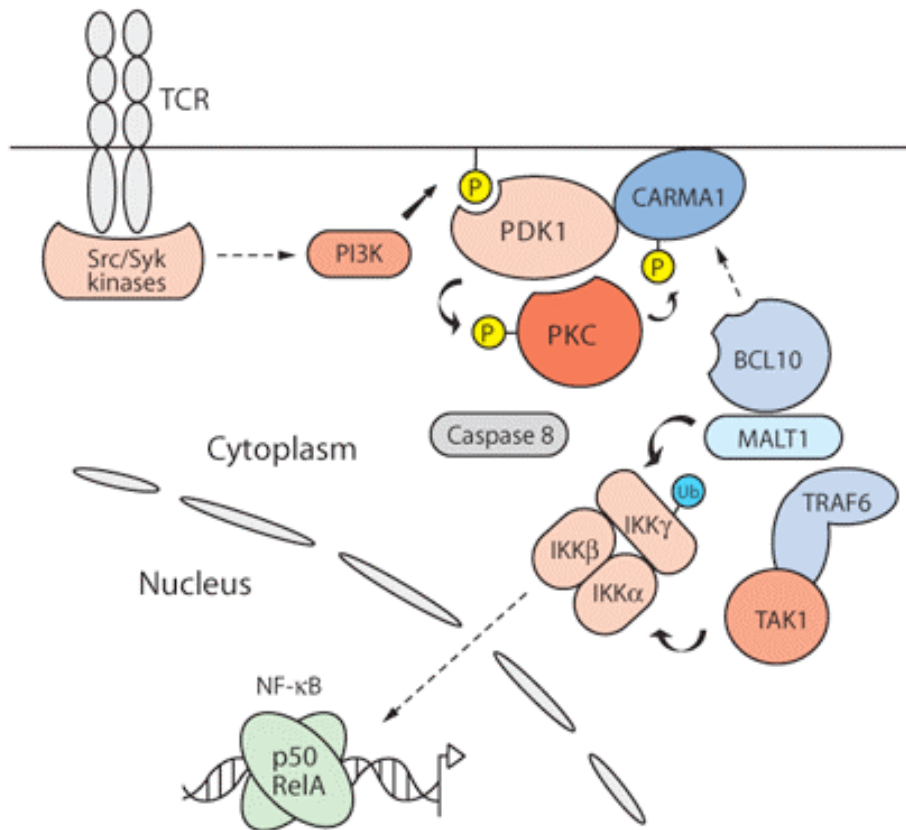


**Figure 9. TCR mediated activation of NF- $\kappa$ B (30).** TCR ligation recruits adaptor proteins such as PI3K and PDK1, which signal to PKC $\theta$ , eventually triggering the formation of the CBM complex. The CBM complex transduces activating signals to the IKK complex via TRAF-6 and TAK1.

Following TCR engagement, the proximal phosphorylation and signaling events at the TCR lead to the formation of diacylglycerol (DAG), a lipid messenger. DAG is thought to bind to the novel PKC family member PKC $\theta$  (Fig. 10), triggering its association with the plasma membrane (reviewed in (31)). At the same time, the activity of PI3K triggers the activation of the kinase PDK1. Activated PDK1 phosphorylates PKC $\theta$  at the membrane, triggering a conformational change in the protein (32).

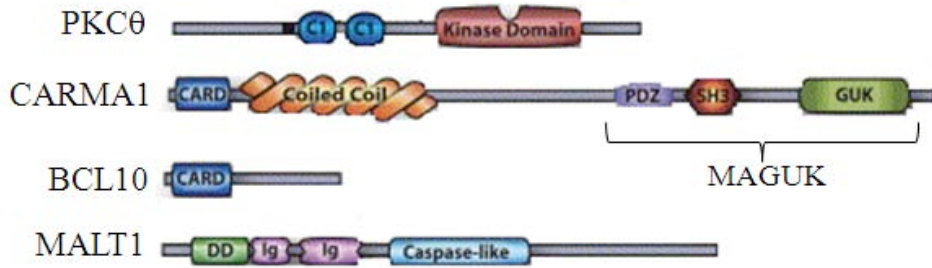


**Figure 10. Structure of PKC $\theta$ , Carma1, Bcl10, and Malt1 (adapted from (20)).** Abbreviations used: CARD – caspase recruitment domain; MAGUK – membrane associated guanylate kinase; DD – death domain; Ig – immunoglobulin domain.

This phosphorylation-induced conformational change allows PKC $\theta$  to interact with and phosphorylate the protein Carma1 (a membrane-associated guanylate kinase) in the hinge region of the protein (Fig. 10) (33, 34). Phosphorylated Carma1 then recruits and binds the protein Bcl10 via CARD-CARD interactions (35, 36). This interaction also recruits the Bcl10 binding partner Malt1 (37) to the membrane, forming the Carma1-Bcl10-Malt1 (CBM) complex. The formation of this complex serves to oligomerize these proteins, creating a nucleation point for further signaling.

Several additional proteins associate with the CBM complex and are involved in signal transduction to NF- $\kappa$ B. The ubiquitin ligase TRAF6 was found to bind to the c-terminus of Malt1 (38). This association results in the oligomerization of TRAF6, which is thought to activate its ubiquitin ligase function. Activated TRAF6 mediates the K63-linked polyubiquitination and activation of the IKK $\gamma$  subunit of the IKK complex. Activated TRAF6 is also thought to ubiquinate the kinase TAK1, causing TAK1 to associate with the IKK complex and phosphorylate and activate IKK $\beta$  (38). Caspase-8 has also been shown to associate with the CBM complex and TRAF6 (39, 40), but the role of this protein in NF- $\kappa$ B activation is not well understood.

Following IKK activation, the terminal NF-κB activation steps proceed as described above.

### ***The function of NF-κB***

As mentioned above, NF-κB controls the expression of a variety of genes, including those involved in cellular proliferation and apoptosis. In terms of proliferation, NF-κB is known to control the expression of many cyclins and cdk proteins (reviewed in (41)). These include the cdk inhibitor p21<sup>waf1/cip1</sup> (42), cyclin D1 (43), and cyclin E (44, 45). Furthermore, NF-κB activity has been linked to the proliferation of various types of cancer cells, ranging from myelomas (46) to breast cancer (47) to esophageal cancer (48), to name a few. NF-κB activation is also implicated in several leukemias and lymphomas, and the signaling proteins Bcl10 and Malt1 were first identified due to chromosomal translocations that resulted in NF-κB activation in MALT lymphomas ((49, 50), respectively).

NF-κB also plays a major role in cellular resistance to apoptosis. NF-κB controls the expression of several anti-apoptotic genes, such as Bcl2 (51, 52), survivin (52), and Bcl-X (45), to name a few. In addition, several studies have shown that inhibition of NF-κB activation renders a B cells more sensitive to apoptotic stimuli (53, 45).

Finally, the importance of NF-κB in the immune system is underscored by the various defects observed in the absence of functional NF-κB signaling (reviewed in (19, 54)). Mice deficient in various NF-κB family members show defects in B cell class switching ( $p65^{-/-}$ ,  $cRel^{-/-}$ , and  $p50^{-/-}$  (55)), abnormal splenic architecture ( $p52^{-/-}$ ), and impaired humoral responses ( $p65^{-/-}$ ,  $RelB^{-/-}$ ,  $cRel^{-/-}$ ,  $p50^{-/-}$ , and  $p52^{-/-}$ ). Furthermore, mice deficient in NF-κB signaling proteins such as PKCθ (56, 57), Bcl10 (58), or Malt1 (59,

60) show impaired T and B cell proliferation and effector function following stimulation. These results underscore the central role of NF- $\kappa$ B in the adaptive immune response.

### ***Introduction to thesis topics***

As described above, many of the major proteins involved in TCR-mediated activation of NF- $\kappa$ B are known. We sought to determine how important some of these proteins are in NF- $\kappa$ B activation by examining TCR-mediated activation of NF- $\kappa$ B in the absence of these proteins. We were particularly interested in how the loss of PKC $\theta$ , Bcl10, or Malt1 would affect TCR signaling to NF- $\kappa$ B. Mice deficient in each of these proteins have been generated by other groups, and the resulting phenotypes are quite interesting. While PKC $\theta^{-/-}$  mice have a normal complement of B cells, T cells from these mice show deficient proliferation and IL-2 production following TCR ligation (56, 57). Close examination of signal transduction events in these cells revealed defective NF- $\kappa$ B and NFAT activation. The immune functions of Bcl10 $^{-/-}$  and Malt1 $^{-/-}$  mice are more affected, as these mice show impaired B cell responses and lower serum immunoglobulin levels (58, 59, 60). Furthermore, Malt1 $^{-/-}$  mice completely lack marginal zone B cells, and Bcl10 $^{-/-}$  mice show impaired development and function of follicular and marginal zone B cells (61). Phenotypically, T cells from Bcl10 $^{-/-}$  and Malt1 $^{-/-}$  mice resemble those from PKC $\theta^{-/-}$  mice, exhibiting impaired proliferation and cytokine responses. However, in terms of signaling to transcription factors, Bcl10 $^{-/-}$  and Malt1 $^{-/-}$  T cells only display a defect in NF- $\kappa$ B activation and retain normal NFAT signaling.

Although T cells from these knock-out animals were characterized as functionally impaired, the above studies did not discriminate between CD4 $^{+}$  and CD8 $^{+}$  T cell responses, and furthermore used limited stimuli to test T cell function. We hypothesized

that knock-out T cells may retain some functional capacity when experiencing strong stimuli, and that CD4<sup>+</sup> and CD8<sup>+</sup> T cells respond differently to the loss of PKCθ, Bcl10, or Malt1. These experiments and the results are described in detail in Chapter 2.

Chapter 3 describes our investigation into the nature of TCR mediated signaling to NF-κB. Specifically, we sought to determine if TCR signaling to NF-κB is digital or analog in nature, a distinction described in greater detail in Chapter 3. Briefly, in digital signaling the output is either ‘on or off’ and the intensity of the output is constant, regardless of the intensity of the input. In contrast, in analog signaling the output is proportional to the input, resulting in a gradation of intensity. Recent reports have described the digital nature of various signaling pathways such as the MAP kinase and Ras pathways, and we sought to determine 1) if NF-κB signaling is digital as well, and 2) if so, at what point does TCR signaling to NF-κB become digital in nature.

Characterizing the digital or analog character of signal transduction cascades may lead to the development of targeted drugs and therapeutics designed to manipulate these important intracellular pathways. If the digitization point of a pathway can be identified, designing inhibitors or activators targeting that step of the pathway would effectively result in an ‘on/off’ switch that would allow for extreme control of the pathway. If more subtle control of the signaling pathway and its effects were desired, manipulating analog signaling events would result in a ‘tunable’ pathway, where signal intensity could be controlled by the amount of inhibitor or activator provided. Given the importance of NF-κB in normal and diseased states, understanding how NF-κB signaling works from a digital or analog perspective will inform the development of therapeutics that better control this key signaling pathway.

## References

1. Charles A. Janeway Jr. , P. T., Mark Walport, Mark J. Shlomchik 2001. Immunobiology: the immune system in health and disease. Garland Publishing, New York.
2. Seder, R. A., and R. Ahmed. 2003. Similarities and differences in CD4+ and CD8+ effector and memory T cell generation. *Nat Immunol* 4:835-842.
3. Ciofani, M., and J. C. Zuniga-Pflucker. 2007. The thymus as an inductive site for T lymphopoiesis. *Annu Rev Cell Dev Biol* 23:463-493.
4. Pitcher, L. A., and N. S. van Oers. 2003. T-cell receptor signal transmission: who gives an ITAM? *Trends Immunol* 24:554-560.
5. Konig, R. 2002. Interactions between MHC molecules and co-receptors of the TCR. *Curr Opin Immunol* 14:75-83.
6. Lucas, P. C., L. M. McAllister-Lucas, and G. Nunez. 2004. NF-kappaB signaling in lymphocytes: a new cast of characters. *J Cell Sci* 117:31-39.
7. van Oers, N. S., N. Killeen, and A. Weiss. 1996. Lck regulates the tyrosine phosphorylation of the T cell receptor subunits and ZAP-70 in murine thymocytes. *J Exp Med* 183:1053-1062.
8. Deindl, S., T. A. Kadlecak, T. Brdicka, X. Cao, A. Weiss, and J. Kuriyan. 2007. Structural basis for the inhibition of tyrosine kinase activity of ZAP-70. *Cell* 129:735-746.
9. Chan, A. C., M. Dalton, R. Johnson, G. H. Kong, T. Wang, R. Thoma, and T. Kurosaki. 1995. Activation of ZAP-70 kinase activity by phosphorylation of tyrosine 493 is required for lymphocyte antigen receptor function. *Embo J* 14:2499-2508.
10. Zhang, W., J. Sloan-Lancaster, J. Kitchen, R. P. Trible, and L. E. Samelson. 1998. LAT: the ZAP-70 tyrosine kinase substrate that links T cell receptor to cellular activation. *Cell* 92:83-92.
11. Wange, R. L. 2000. LAT, the Linker for Activation of T Cells: A Bridge Between T Cell-Specific and General Signaling Pathways *Science STKE* 2000.
12. Bubeck Wardenburg, J., C. Fu, J. K. Jackman, H. Flotow, S. E. Wilkinson, D. H. Williams, R. Johnson, G. Kong, A. C. Chan, and P. R. Findell. 1996. Phosphorylation of SLP-76 by the ZAP-70 protein-tyrosine kinase is required for T-cell receptor function. *J Biol Chem* 271:19641-19644.
13. Rao, A., C. Luo, and P. G. Hogan. 1997. Transcription factors of the NFAT family: regulation and function. *Annu Rev Immunol* 15:707-747.
14. Hogan, P. G., L. Chen, J. Nardone, and A. Rao. 2003. Transcriptional regulation by calcium, calcineurin, and NFAT. *Genes Dev* 17:2205-2232.
15. Macian, F. 2005. NFAT proteins: key regulators of T-cell development and function. *Nat Rev Immunol* 5:472-484.
16. Angel, P., and M. Karin. 1991. The role of Jun, Fos and the AP-1 complex in cell-proliferation and transformation. *Biochim Biophys Acta* 1072:129-157.

17. Ho, N., M. Gullberg, and T. Chatila. 1996. Activation protein 1-dependent transcriptional activation of interleukin 2 gene by Ca<sup>2+</sup>/calmodulin kinase type IV/Gr. *J Exp Med* 184:101-112.
18. Sen, R., and D. Baltimore. 1986. Multiple nuclear factors interact with the immunoglobulin enhancer sequences. *Cell* 46:705-716.
19. Hayden, M. S., and S. Ghosh. 2004. Signaling to NF-kappaB. *Genes Dev* 18:2195-2224.
20. Schulze-Luehrmann, J., and S. Ghosh. 2006. Antigen-receptor signaling to nuclear factor kappa B. *Immunity* 25:701-715.
21. Ghosh, S., and M. S. Hayden. 2008. New regulators of NF-kappaB in inflammation. *Nat Rev Immunol* 8:837-848.
22. Mercurio, F., H. Zhu, B. W. Murray, A. Shevchenko, B. L. Bennett, J. Li, D. B. Young, M. Barbosa, M. Mann, A. Manning, and A. Rao. 1997. IKK-1 and IKK-2: cytokine-activated IkappaB kinases essential for NF-kappaB activation. *Science* 278:860-866.
23. DiDonato, J., F. Mercurio, C. Rosette, J. Wu-Li, H. Suyang, S. Ghosh, and M. Karin. 1996. Mapping of the inducible IkappaB phosphorylation sites that signal its ubiquitination and degradation. *Mol Cell Biol* 16:1295-1304.
24. Brown, K., S. Park, T. Kanno, G. Franzoso, and U. Siebenlist. 1993. Mutual regulation of the transcriptional activator NF-kappa B and its inhibitor, I kappa B-alpha. *Proc Natl Acad Sci U S A* 90:2532-2536.
25. Sun, S. C., P. A. Ganchi, D. W. Ballard, and W. C. Greene. 1993. NF-kappa B controls expression of inhibitor I kappa B alpha: evidence for an inducible autoregulatory pathway. *Science* 259:1912-1915.
26. Liu, Y. C., J. Penninger, and M. Karin. 2005. Immunity by ubiquitylation: a reversible process of modification. *Nat Rev Immunol* 5:941-952.
27. Chen, Z. J. 2005. Ubiquitin signalling in the NF-kappaB pathway. *Nat Cell Biol* 7:758-765.
28. Xiao, G., A. B. Rabson, W. Young, G. Qing, and Z. Qu. 2006. Alternative pathways of NF-kappaB activation: a double-edged sword in health and disease. *Cytokine Growth Factor Rev* 17:281-293.
29. Senftleben, U., Y. Cao, G. Xiao, F. R. Greten, G. Krahn, G. Bonizzi, Y. Chen, Y. Hu, A. Fong, S. C. Sun, and M. Karin. 2001. Activation by IKKalpha of a second, evolutionary conserved, NF-kappa B signaling pathway. *Science* 293:1495-1499.
30. Hacker, H., and M. Karin. 2006. Regulation and function of IKK and IKK-related kinases. *Sci STKE* 2006:re13.
31. Hayashi, K., and A. Altman. 2007. Protein kinase C theta (PKCtheta): a key player in T cell life and death. *Pharmacol Res* 55:537-544.
32. Lee, K. Y., F. D'Acquisto, M. S. Hayden, J. H. Shim, and S. Ghosh. 2005. PDK1 nucleates T cell receptor-induced signaling complex for NF-kappaB activation. *Science* 308:114-118.
33. Matsumoto, R., D. Wang, M. Blonska, H. Li, M. Kobayashi, B. Pappu, Y. Chen, D. Wang, and X. Lin. 2005. Phosphorylation of CARMA1 plays a critical role in T Cell receptor-mediated NF-kappaB activation. *Immunity* 23:575-585.

34. Sommer, K., B. Guo, J. L. Pomerantz, A. D. Bandaranayake, M. E. Moreno-Garcia, Y. L. Ovechkina, and D. J. Rawlings. 2005. Phosphorylation of the CARMA1 linker controls NF-kappaB activation. *Immunity* 23:561-574.
35. Gaide, O., F. Martinon, O. Micheau, D. Bonnet, M. Thome, and J. Tschopp. 2001. Carma1, a CARD-containing binding partner of Bcl10, induces Bcl10 phosphorylation and NF-kappaB activation. *FEBS Lett* 496:121-127.
36. Gaide, O., B. Favier, D. F. Legler, D. Bonnet, B. Brissoni, S. Valitutti, C. Bron, J. Tschopp, and M. Thome. 2002. CARMA1 is a critical lipid raft-associated regulator of TCR-induced NF-kappa B activation. *Nat Immunol* 3:836-843.
37. Lucas, P. C., M. Yonezumi, N. Inohara, L. M. McAllister-Lucas, M. E. Abazeed, F. F. Chen, S. Yamaoka, M. Seto, and G. Nunez. 2001. Bcl10 and MALT1, independent targets of chromosomal translocation in malt lymphoma, cooperate in a novel NF-kappa B signaling pathway. *J Biol Chem* 276:19012-19019.
38. Sun, L., L. Deng, C. K. Ea, Z. P. Xia, and Z. J. Chen. 2004. The TRAF6 ubiquitin ligase and TAK1 kinase mediate IKK activation by BCL10 and MALT1 in T lymphocytes. *Mol Cell* 14:289-301.
39. Bidere, N., A. L. Snow, K. Sakai, L. Zheng, and M. J. Lenardo. 2006. Caspase-8 regulation by direct interaction with TRAF6 in T cell receptor-induced NF-kappaB activation. *Curr Biol* 16:1666-1671.
40. Misra, R. S., J. Q. Russell, A. Koenig, J. A. Hinshaw-Makepeace, R. Wen, D. Wang, H. Huo, D. R. Littman, U. Ferch, J. Ruland, M. Thome, and R. C. Budd. 2007. Caspase-8 and c-FLIPL associate in lipid rafts with NF-kappaB adaptors during T cell activation. *J Biol Chem* 282:19365-19374.
41. Joyce, D., C. Albanese, J. Steer, M. Fu, B. Bouzahzah, and R. G. Pestell. 2001. NF-kappaB and cell-cycle regulation: the cyclin connection. *Cytokine Growth Factor Rev* 12:73-90.
42. Wuerzberger-Davis, S. M., P. Y. Chang, C. Berchtold, and S. Miyamoto. 2005. Enhanced G2-M arrest by nuclear factor- $\{\kappa\}$ B-dependent p21waf1/cip1 induction. *Mol Cancer Res* 3:345-353.
43. Hinz, M., D. Krappmann, A. Eichten, A. Heder, C. Scheidereit, and M. Strauss. 1999. NF-kappaB function in growth control: regulation of cyclin D1 expression and G0/G1-to-S-phase transition. *Mol Cell Biol* 19:2690-2698.
44. Hsia, C. Y., S. Cheng, A. M. Owyang, S. F. Dowdy, and H. C. Liou. 2002. c-Rel regulation of the cell cycle in primary mouse B lymphocytes. *Int Immunol* 14:905-916.
45. Feng, B., S. Cheng, C. Y. Hsia, L. B. King, J. G. Monroe, and H. C. Liou. 2004. NF-kappaB inducible genes BCL-X and cyclin E promote immature B-cell proliferation and survival. *Cell Immunol* 232:9-20.
46. Li, Z. W., H. Chen, R. A. Campbell, B. Bonavida, and J. R. Berenson. 2008. NF-kappaB in the pathogenesis and treatment of multiple myeloma. *Curr Opin Hematol* 15:391-399.
47. Sovak, M. A., R. E. Bellas, D. W. Kim, G. J. Zanieski, A. E. Rogers, A. M. Traish, and G. E. Sonenshein. 1997. Aberrant nuclear factor-kappaB/Rel expression and the pathogenesis of breast cancer. *J Clin Invest* 100:2952-2960.
48. Abdel-Latif, M. M., J. O'Riordan, H. J. Windle, E. Carton, N. Ravi, D. Kelleher, and J. V. Reynolds. 2004. NF-kappaB activation in esophageal adenocarcinoma:

- relationship to Barrett's metaplasia, survival, and response to neoadjuvant chemoradiotherapy. *Ann Surg* 239:491-500.
49. Willis, T. G., D. M. Jadayel, M. Q. Du, H. Peng, A. R. Perry, M. Abdul-Rauf, H. Price, L. Karran, O. Majekodunmi, I. Wlodarska, L. Pan, T. Crook, R. Hamoudi, P. G. Isaacson, and M. J. Dyer. 1999. Bcl10 is involved in t(1;14)(p22;q32) of MALT B cell lymphoma and mutated in multiple tumor types. *Cell* 96:35-45.
  50. Akagi, T., M. Motegi, A. Tamura, R. Suzuki, Y. Hosokawa, H. Suzuki, H. Ota, S. Nakamura, Y. Morishima, M. Taniwaki, and M. Seto. 1999. A novel gene, MALT1 at 18q21, is involved in t(11;18) (q21;q21) found in low-grade B-cell lymphoma of mucosa-associated lymphoid tissue. *Oncogene* 18:5785-5794.
  51. Zong, W. X., L. C. Edelstein, C. Chen, J. Bash, and C. Gelinas. 1999. The prosurvival Bcl-2 homolog Bfl-1/A1 is a direct transcriptional target of NF-kappaB that blocks TNFalpha-induced apoptosis. *Genes Dev* 13:382-387.
  52. Song, J., T. So, and M. Croft. 2008. Activation of NF-kappaB1 by OX40 contributes to antigen-driven T cell expansion and survival. *J Immunol* 180:7240-7248.
  53. Wu, M., H. Lee, R. E. Bellas, S. L. Schauer, M. Arsura, D. Katz, M. J. FitzGerald, T. L. Rothstein, D. H. Sherr, and G. E. Sonenshein. 1996. Inhibition of NF-kappaB/Rel induces apoptosis of murine B cells. *Embo J* 15:4682-4690.
  54. Hayden, M. S., A. P. West, and S. Ghosh. 2006. NF-kappaB and the immune response. *Oncogene* 25:6758-6780.
  55. Snapper, C. M., P. Zelazowski, F. R. Rosas, M. R. Kehry, M. Tian, D. Baltimore, and W. C. Sha. 1996. B cells from p50/NF-kappa B knockout mice have selective defects in proliferation, differentiation, germ-line CH transcription, and Ig class switching. *J Immunol* 156:183-191.
  56. Pfeifhofer, C., K. Kofler, T. Gruber, N. G. Tabrizi, C. Lutz, K. Maly, M. Leitges, and G. Baier. 2003. Protein kinase C theta affects Ca2+ mobilization and NFAT cell activation in primary mouse T cells. *J Exp Med* 197:1525-1535.
  57. Sun, Z., C. W. Arendt, W. Ellmeier, E. M. Schaeffer, M. J. Sunshine, L. Gandhi, J. Annes, D. Petrzelka, A. Kupfer, P. L. Schwartzberg, and D. R. Littman. 2000. PKC-theta is required for TCR-induced NF-kappaB activation in mature but not immature T lymphocytes. *Nature* 404:402-407.
  58. Ruland, J., G. S. Duncan, A. Elia, I. del Barco Barrantes, L. Nguyen, S. Plyte, D. G. Millar, D. Bouchard, A. Wakeham, P. S. Ohashi, and T. W. Mak. 2001. Bcl10 is a positive regulator of antigen receptor-induced activation of NF-kappaB and neural tube closure. *Cell* 104:33-42.
  59. Ruland, J., G. S. Duncan, A. Wakeham, and T. W. Mak. 2003. Differential requirement for Malt1 in T and B cell antigen receptor signaling. *Immunity* 19:749-758.
  60. Ruefli-Brasse, A. A., D. M. French, and V. M. Dixit. 2003. Regulation of NF-kappaB-dependent lymphocyte activation and development by paracaspase. *Science* 302:1581-1584.
  61. Xue, L., S. W. Morris, C. Orihuela, E. Tuomanen, X. Cui, R. Wen, and D. Wang. 2003. Defective development and function of Bcl10-deficient follicular, marginal zone and B1 B cells. *Nat Immunol* 4:857-865.

**Chapter 2: Loss of Protein Kinase C $\theta$ , Bcl10, or Malt1 Selectively Impairs  
Proliferation and NF- $\kappa$ B Activation in the CD4 $^+$  T Cell Subset.**

**Lara M. Kingeter and Brian C. Schaefer**

*Published in the Journal of Immunology, 2008, 181(9): 6244-54*

# Loss of Protein Kinase C $\theta$ , Bcl10, or Malt1 Selectively Impairs Proliferation and NF- $\kappa$ B Activation in the CD4 $^{+}$ T Cell Subset<sup>1</sup>

Lara M. Kingeter and Brian C. Schaefer<sup>2</sup>

The cytosolic proteins protein kinase C $\theta$  (PKC $\theta$ ), Bcl10, and Malt1 play critical roles in TCR signaling to the transcription factor NF- $\kappa$ B. Our data confirm that CD4 $^{+}$  T cells from PKC $\theta$ , Bcl10, and Malt1 knockout mice show severe impairment of proliferation in response to TCR stimulation. Unexpectedly, we find that knockout CD8 $^{+}$  T cells proliferate to a similar extent as wild-type cells in response to strong TCR signals, although a survival defect prevents their accumulation. Both CD4 $^{+}$  and CD8 $^{+}$  knockout T cells express activation markers, including CD25, following TCR stimulation. Addition of exogenous IL-2 rescues survival of knockout CD4 $^{+}$  and CD8 $^{+}$  T cells, but fails to overcome the proliferation defect of CD4 $^{+}$  T cells. CD4 $^{+}$  T cells from knockout mice are extremely deficient in TCR-induced NF- $\kappa$ B activation, whereas NF- $\kappa$ B activation is only partially impaired in CD8 $^{+}$  T cells. Overall, our results suggest that defects in TCR signaling through PKC $\theta$ , Bcl10, and Malt1 predominantly impair NF- $\kappa$ B activation and downstream functional responses of CD4 $^{+}$  T cells. In contrast, CD8 $^{+}$  T cells maintain substantial NF- $\kappa$ B signaling, implying the existence of a significant TCR-regulated NF- $\kappa$ B activation pathway in CD8 $^{+}$  T cells that is independent of PKC $\theta$ , Bcl10, and Malt1. *The Journal of Immunology*, 2008, 181: 6244–6254.

**T** cell activation is initiated when the TCR encounters cognate peptide:MHC displayed on the surface of an APC. Engagement of the TCR initiates a series of signal transduction events that culminate in T cell proliferation and gain of effector functions. One of the key transcription factors activated during this process is NF- $\kappa$ B, which is a central regulator of numerous genes involved in T cell survival, proliferation, and effector function.

NF- $\kappa$ B activation is a tightly controlled process (reviewed in Refs. 1–3). In the absence of stimulation, NF- $\kappa$ B is retained in the cytoplasm through its association with I $\kappa$ B proteins, an interaction that masks the nuclear localization sequence of NF- $\kappa$ B. Following TCR engagement, protein kinase C $\theta$  (PKC $\theta$ )<sup>3</sup>, a novel protein kinase C enzyme, is activated and phosphorylates Carmal, a CARD-containing MAGUK protein (4, 5). Carmal then associates with a preexisting complex, consisting of the CARD protein Bcl10 and the caspase-like protein Malt1, to form the Carmal-Bcl10-Malt1 complex (6–8). Through its association with TNFR-associated factor 6, Malt1 then effects K63-linked polyubiquitination of the regulatory  $\gamma$  subunit of the I $\kappa$ B kinase (IKK) complex (9, 10). Caspase 8 is also required

for IKK activation, both via stabilizing IKK interaction with Bcl10 and Malt1 (11) and via recruiting Bcl10 and Malt1 to lipid rafts (12). K63-ubiquitinated IKK $\gamma$  serves as a docking site for the kinase TAK1, which phosphorylates and activates IKK $\beta$  (9). Activated IKK $\beta$  phosphorylates I $\kappa$ B, leading to its subsequent K48-linked polyubiquitination and proteasomal destruction (13). NF- $\kappa$ B then enters the nucleus, where it controls the transcription of target genes.

Mice deficient in PKC $\theta$ , Bcl10, and Malt1 have been generated and characterized (14–19). T cells from these knockout animals exhibit very similar phenotypes, including impaired NF- $\kappa$ B activation, deficient IL-2 production, reduced expression of activation markers, and diminished cell proliferation in response to TCR ligation. Overall, these previous studies suggest that PKC $\theta^{-/-}$ , Bcl10 $^{-/-}$ , and Malt1 $^{-/-}$  T cells are essentially nonfunctional. However, a more recent study has shown that PKC $\theta^{-/-}$  mice are able to mount effective CD8 $^{+}$  T cell responses to some viral infections (20), challenging the model that T cells are nonfunctional in the absence of PKC $\theta$ , Bcl10, or Malt1. We have therefore re-examined the responses of these knockout T cells, using more robust TCR stimulation than was used in the original studies of these animals (14–19).

Our results confirm previous findings demonstrating that the loss of PKC $\theta$ , Bcl10, or Malt1 severely impacts CD4 $^{+}$  T cell proliferation. Surprisingly, however, we find that under conditions of strong TCR stimulation, CD8 $^{+}$  T cells from knockout mice proliferate to a similar extent as wild-type (WT) cells, although a survival defect limits their accumulation. Both CD4 $^{+}$  and CD8 $^{+}$  knockout T cells up-regulate CD25 and CD44 in response to strong TCR stimulation, but these cells are highly deficient in IL-2 production. Addition of exogenous IL-2 improves knockout T cell survival, but does not restore knockout CD4 $^{+}$  T cell proliferation. CD4 $^{+}$  T cells from knockout mice fail to activate NF- $\kappa$ B in response to TCR ligation, whereas a subset of CD8 $^{+}$  T cells from these animals successfully activate NF- $\kappa$ B. Our results suggest that although CD4 $^{+}$  T cells are highly dependent on PKC $\theta$ , Bcl10, and Malt1 to fully activate NF- $\kappa$ B in response to TCR ligation, CD8 $^{+}$

Department of Microbiology and Immunology, Uniformed Services University, Bethesda, MD 20814

Received for publication January 2, 2008. Accepted for publication September 3, 2008.

The costs of publication of this article were defrayed in part by the payment of page charges. This article must therefore be hereby marked *advertisement* in accordance with 18 U.S.C. Section 1734 solely to indicate this fact.

<sup>1</sup> Funding for this project was provided by grants to B.C.S. from the National Institutes of Health/National Institute of Allergy and Infectious Diseases (AI057481), the Sidney Kimmel Foundation for Cancer Research, and the Dana Foundation.

<sup>2</sup> Address correspondence and reprint requests to Dr. Brian C. Schaefer, Department of Microbiology and Immunology, Uniformed Services University, 4301 Jones Bridge Road, Room B3104, Bethesda, MD 20814-4799. E-mail address: bschaefer@usuhs.mil

<sup>3</sup> Abbreviations used in this paper: PKC $\theta$ , protein kinase C $\theta$ ; IKK, I $\kappa$ B kinase; WT, wild type; EHAA, Eagle's Ham's Amino Acids; PI, propidium iodide; rm, recombinant mouse.

T cells are able to utilize an uncharacterized parallel pathway to successfully activate NF- $\kappa$ B and drive T cell proliferation in the absence of these molecules.

## Materials and Methods

### Mice

Tissues were harvested from 6- to 10-wk-old C57BL/6 (WT) mice (National Cancer Institute), Bcl10 $^{-/-}$ , and Malt1 $^{-/-}$  mice (16, 17) (provided by T. Mak, University of Toronto, Toronto, Canada), and PKC $\theta^{-/-}$  mice (18) (provided by A. Kupfer, Johns Hopkins University School of Medicine, Baltimore, MD). Bcl10 $^{-/-}$  and PKC $\theta^{-/-}$  mice were backcrossed with C57BL/6 mice for at least five generations. For TCR-transgenic experiments, tissues were harvested from 4- to 7-wk-old OTII (21), HY (22), PKC $\theta^{-/-}$  OTII, and PKC $\theta^{-/-}$  HY mice. All mouse experiments were approved by the Uniformed Services University of Health Science Institutional Animal Care and Use Committee.

### T cell purification and culture

Lymph nodes were collected in ice-cold HBSS and passed through a 70- $\mu$ m cell strainer to create a single-cell suspension. T cells were isolated by negative selection using biotinylated Abs to B220 (RA3-6B2), CD11b (M1/70), FC $\gamma$ R (2.4G2), and MHC class II (KHT4), followed by incubation and separation with streptavidin-coated magnetic beads (Dynal), resulting in T cell purities of 95–98%. To purify CD4 $^{+}$  T cells, biotin anti-CD8 (53-6.7; BioLegend) was added to the above Ab combination, resulting in CD4 $^{+}$  purities of 98% or greater. To purify CD8 $^{+}$  T cells, biotin anti-CD4 (GK1.5) was added, resulting in CD8 $^{+}$  purities of 94% or greater. Cells were rested for an average of 2.5 h (range, 1 h 45 min to 4 h) before plating by incubation in Eagle's Ham's Amino Acids (EHAA) medium. For some experiments, cells were rested in EHAA medium supplemented with 5 ng/ml recombinant mouse (rm) IL-7 (see Figs. 1, A and C–E, and 6, C–F). T cell cultures received 1  $\mu$ g/ml anti-CD28 (37.51; BD Pharmingen) unless otherwise indicated.

### T cell proliferation

A 96-well plate was coated overnight at 4°C with the indicated concentrations of anti-TCR $\beta$  (H597), followed by six washes with HBSS. Purified T cells were labeled with CFSE (1 mM) and plated at a density of 3–4  $\times$  10 $^5$  cells/well in 100–200  $\mu$ l of EHAA medium (Invitrogen). At the indicated times, cells were stained with anti-CD4 allophycocyanin (RM4-5; Caltag Laboratories) and anti-CD8 PerCP (53-6.7; BD Pharmingen), and CFSE dilution was assessed by flow cytometry. In some experiments (see Figs. 4 and 5), cells were supplemented with recombinant murine IL-2 (R&D Systems) at 2 or 50 ng/ml after 24 h of culture.

For assessment of Ag-stimulated proliferation, C57BL/6 splenocytes were treated with mitomycin C (40  $\mu$ g/ml) and 1  $\times$  10 $^5$  cells were plated in a 96-well plate. Lymphocytes were isolated from OTII or HY TCR-transgenic mice, labeled with CFSE, and 4  $\times$  10 $^5$  lymphocytes were cultured with peptide-pulsed splenocytes. WT OVA<sub>325–339</sub> (QAVHAA-HAEINEAGR) or the OVA 331K (23) nonstimulatory (null) variant was used to stimulate OTII T cells, and SMCY (738–746) (KCSRNRQYL) or the null variant SMCY 743A (24) was used to stimulate HY T cells. Cells were harvested every 24 h and stained with anti-CD4 allophycocyanin (RM4-5; Caltag Laboratories) and anti-V $\beta$ 5 PE (MR9-4; BD Pharmingen) to identify OTII T cells, or with anti-CD8 Alexa Fluor 647 (53-6.7) and anti-V $\beta$ 8 PE (F23.1; BD Pharmingen) to identify HY T cells.

Flow cytometry was performed on a Beckman Coulter LSRII, and data analysis was performed using WinList 5.0. The proliferation index for CFSE-labeled cells was calculated using ModFit software (version 3.1, service pack 3; Verity Software House).

### Western blotting

Primary C57BL/6 or PKC $\theta^{-/-}$  T cells were purified with Celllect T cell columns (Cedarlane Laboratories) and stimulated with plate-bound anti-CD3 $\epsilon$  plus soluble anti-CD28. Whole cell lysates were prepared on ice by direct lysis of cells and sonication in 1  $\times$  Laemmli buffer. Protein lysates were separated by SDS-PAGE and blotted onto nitrocellulose membranes. Proteins were detected by a mAb against PKC $\theta$  (BD Pharmingen) and polyclonal Abs against phospho-I $\kappa$ B $\alpha$  (Ser-32; Cell Signaling Technologies), cyclin E, and actin (both from Santa Cruz Biotechnology). Proteins were detected by chemiluminescence using HRP-conjugated secondary Abs, except for actin, which was detected by direct fluorescence of a Cy3-conjugated secondary Ab.

### Phospho-I $\kappa$ B $\alpha$ staining

Stimulated T cells were harvested and stained with anti-CD4 PE (GK1.5; eBioscience) and anti-CD8 PerCP (53-6.7; BD Pharmingen). Cells were washed twice, fixed, and permeabilized. Phospho-I $\kappa$ B $\alpha$  was detected by overnight incubation at 4°C with a rabbit polyclonal Ab (Ser-32; Cell Signaling Technology), followed by a 30-min incubation with Alexa Fluor 647 goat anti-rabbit IgG (Molecular Probes) and flow cytometry analysis. Experiments conducted with a rabbit mAb to phospho-I $\kappa$ B $\alpha$  (Ser-32; Cell Signaling Technology) yielded similar results. For experiments with IKK inhibitors, T cells were treated at 48 h after TCR stimulation with 5  $\mu$ g/ml BAY11-7082 or BAY11-7085 (Calbiochem) in DMSO or with an equivalent volume of DMSO or EHAA medium. Cells were harvested after 30 min and 2 h, and phospho-I $\kappa$ B $\alpha$  was detected as described above.

### Epifluorescence microscopy

Purified T cells were harvested every 24 h and stained with anti-CD4 Oregon Green (GK1.5) and anti-CD8 Alexa Fluor 647 (53-6.7). Cells were placed on poly-D-lysine-coated coverslips and incubated at 37°C for 5 min. Cells were fixed, permeabilized, blocked, and stained with rabbit anti-NF- $\kappa$ B p65 (C-20; Santa Cruz Biotechnology), followed by Alexa Fluor 555 goat anti-rabbit (Molecular Probes) and 4,6'-diamidino-2-phenylindole (Molecular Probes). Fluorescence images were collected and deconvolved using a Zeiss Axiovert 200M/TILL Photonics imaging system as previously described (25). Three deconvolved images, representing the approximate middle of the cell (0.9  $\mu$ M cross-section) were combined using a maximal projection algorithm. Regions of interest were drawn in the nucleus and cytoplasm of cells (using 4,6'-diamidino-2-phenylindole staining to define the nucleus), and the mean pixel intensity was calculated. After correcting for background fluorescence, the nuclear p65:cytoplasmic p65 ratio was calculated.

### Analysis of apoptosis and cell surface markers

T cells were purified and divided into two populations. CFSE-labeled cells were plated on anti-TCR $\beta$  as described above, then harvested every 24 h and stained with anti-CD4 allophycocyanin Cy7 (GK1.5; BD Pharmingen) and anti-CD8 Alexa Fluor 647 (53-6.7), followed by subsequent staining with Hoechst 33342 and propidium iodide (PI), according to the manufacturer's instructions (Molecular Probes). Cells were analyzed by flow cytometry and total apoptosis was calculated by adding the percentage of cells with loss of membrane integrity (PI bright) to the percentage of cells with subgenomic DNA content (PI-excluding cells with <2n DNA content, as determined by Hoechst 33342 staining). High apoptosis at t = 0 was consistent and was due to cell death during the harvesting and purification procedures. All events were included in the FACS gating. For detection of cell surface markers, unlabeled T cells were plated on anti-TCR $\beta$ , harvested every 24 h, and stained with anti-CD4 allophycocyanin (RM4-5; Caltag Laboratories), anti-CD8 Alexa Fluor 647 (53-6.7), anti-CD25 PE (PC61; BD Pharmingen) and anti-CD44 FITC (IM7; eBioscience).

### Analysis of apoptosis in divided cells

T cells were purified, labeled with CFSE, and stimulated with 100  $\mu$ g/ml plate-bound anti-TCR $\beta$ . After 24 h, rmIL-2 (R&D Systems) was added at 2 and 50 ng/ml. Cells were harvested every 24 h and stained with annexin V-allophycocyanin (BD Biosciences) according to the manufacturer's instructions. CFSE dilution was assessed in CD8 $^{+}$  T cells and the percentage of annexin V $^{\text{high}}$  cells in the parent and divided cell populations was determined.

### IL-2 ELISA

ELISAs were performed using rat anti-mouse IL-2 capture Ab and biotinylated goat anti-mouse IL-2 detection Ab (R&D Systems). Data were analyzed using the MKASSAY program developed by J. Kappler (Howard Hughes Medical Institute, Denver, CO).

## Results

### *CD4 $^{+}$ T cells from PKC $\theta^{-/-}$ , Bcl10 $^{-/-}$ , and Malt1 $^{-/-}$ mice fail to proliferate in response to TCR stimulation*

To assess the proliferative capacity of CD4 $^{+}$  and CD8 $^{+}$  T cells from WT, PKC $\theta^{-/-}$ , Bcl10 $^{-/-}$ , and Malt1 $^{-/-}$  mice under conditions simulating a strong Ag signal, purified T cells were labeled with CFSE and stimulated with 10–100  $\mu$ g/ml plate-bound

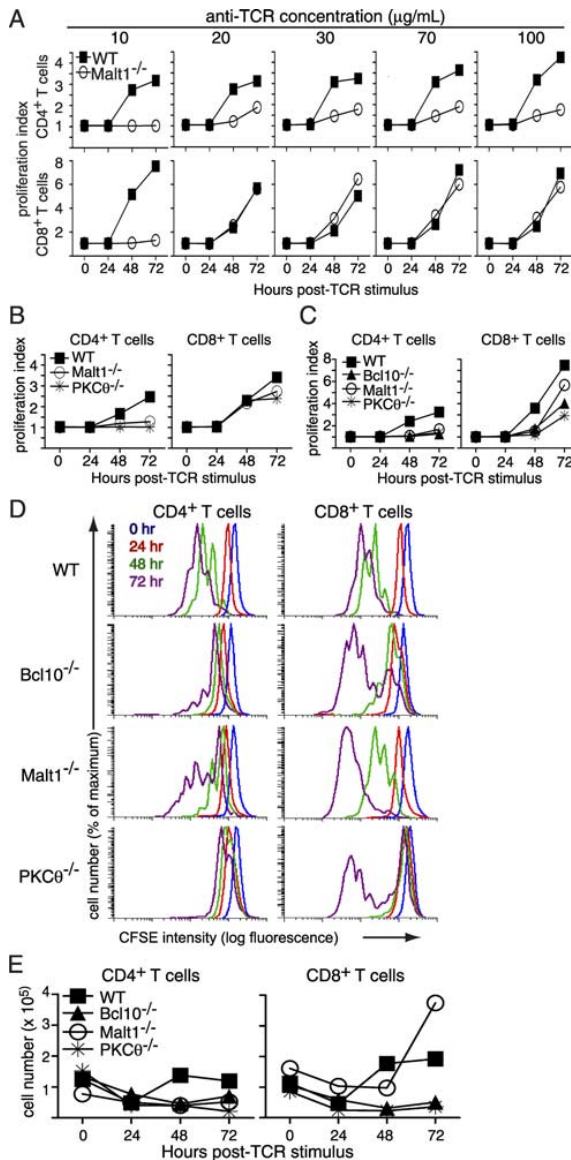


**FIGURE 1.** CD4<sup>+</sup> T cells from PKC $\theta^{-/-}$ , Bcl10 $^{-/-}$ , and Malt1 $^{-/-}$  mice fail to proliferate in response to TCR stimulation. Purified T cells from the indicated strains of mice were labeled with CFSE and stimulated with plate-bound anti-TCR $\beta$  at the indicated concentrations (A), 100  $\mu$ g/ml (B), and 30  $\mu$ g/ml (C). Proliferation was assessed every 24 h by flow cytometry. D, Primary CFSE histogram data from the experiment shown in C. Overlays show the dilution of CFSE in CD4<sup>+</sup> and CD8<sup>+</sup> T cells over time. E, Total numbers of live T cells from the experiment in C were quantified by trypan blue staining. Data in A are representative of two experiments performed at similar doses of anti-TCR $\beta$  stimulation, while data in B–E are representative of four experiments performed with 30–100  $\mu$ g/ml anti-TCR $\beta$  stimulation.

anti-TCR $\beta$ . As shown in Fig. 1A, CD4<sup>+</sup> T cells from Malt1 $^{-/-}$  mice show little to no proliferation in response to a range of anti-TCR $\beta$  concentrations, while WT CD4<sup>+</sup> T cells show modest proliferation in response to the lowest tested doses of anti-TCR $\beta$  (10 and 20  $\mu$ g/ml) and robust proliferation in response to higher concentrations of plate-bound anti-TCR $\beta$  (30–100  $\mu$ g/ml). Surprisingly, although Malt1 $^{-/-}$  CD8<sup>+</sup> T cells did not proliferate in re-

sponse to the lowest concentration of anti-TCR $\beta$  (10  $\mu$ g/ml), these cells exhibited WT levels of proliferation in response to all other concentrations of anti-TCR $\beta$  (20–100  $\mu$ g/ml).

To determine whether these proliferative differences could also be generalized to T cells from PKC $\theta^{-/-}$  and Bcl10 $^{-/-}$  mice, we stimulated PKC $\theta^{-/-}$  and Bcl10 $^{-/-}$  T cells with plate-bound anti-TCR $\beta$  and examined proliferation, relative to WT T cells. Consistent with the response of Malt1 $^{-/-}$  cells, CD4<sup>+</sup> T cells from PKC $\theta^{-/-}$  mice showed little to no proliferation following anti-TCR $\beta$  stimulation, while PKC $\theta^{-/-}$  CD8<sup>+</sup> T cells proliferated to almost the same extent as WT cells (Fig. 1B). In a side-by-side comparison of proliferation, CD4<sup>+</sup> T cells from PKC $\theta^{-/-}$ , Bcl10 $^{-/-}$ , and Malt1 $^{-/-}$  mice exhibited a strong proliferative defect, relative to WT cells, following TCR ligation. In contrast, CD8<sup>+</sup> T cells from these animals proliferated modestly, although not as well as WT cells in this experiment (Fig. 1C). Interestingly, there was a gradation of proliferative responses among the knockout CD8<sup>+</sup> T cells, with Malt1 $^{-/-}$  CD8<sup>+</sup> T cells proliferating to a greater extent than Bcl10 $^{-/-}$  CD8<sup>+</sup> T cells, and PKC $\theta^{-/-}$  CD8<sup>+</sup> T cells showing the least robust proliferation.

Examination of the primary CFSE data (Fig. 1D) revealed that the proliferating PKC $\theta^{-/-}$ , Bcl10 $^{-/-}$ , and Malt1 $^{-/-}$  CD8<sup>+</sup> T cells generally underwent as many divisions as the WT CD8<sup>+</sup> T cells. However, in contrast to WT cells, there was also a significant population of CD8<sup>+</sup> T cells from the knockout animals that did not divide at all. In contrast, CD4<sup>+</sup> T cells from PKC $\theta^{-/-}$ , Bcl10 $^{-/-}$ , and Malt1 $^{-/-}$  mice not only had a larger population of cells that failed to divide, but they also divided fewer times than their WT counterparts. Once again, there was a gradation in the severity of the proliferative defect, with PKC $\theta^{-/-}$  T cells being the most impaired and Malt1 $^{-/-}$  T cells being the least impaired.

Consistent with the proliferation data, the number of live knockout CD4<sup>+</sup> T cells in culture declined over the course of 72 h (Fig. 1E). Interestingly, the number of live Bcl10 $^{-/-}$  and PKC $\theta^{-/-}$  CD8<sup>+</sup> T cells in culture also declined during the experiment, suggesting that although these cells proliferate vigorously, they may have a survival defect. Notably, the CD8<sup>+</sup> Malt1 $^{-/-}$  T cells showed a dramatic increase in total cell numbers between 48 and 72 h, demonstrating that these T cells successfully expand in culture, although with delayed kinetics. Overall, these data demonstrate that the loss of PKC $\theta$ , Bcl10, or Malt1 differentially affects the proliferation of CD4<sup>+</sup> and CD8<sup>+</sup> T cells, with CD4<sup>+</sup> T cells being severely affected under all conditions of stimulation, whereas CD8<sup>+</sup> T cells show little to no proliferative deficiency under conditions of strong stimulation through the TCR.

#### PKC $\theta$ is required for Ag-stimulated proliferation of CD4<sup>+</sup>, but not CD8<sup>+</sup>, T cells

To ensure that the results presented in Fig. 1 did not reflect an artifact of using high levels of anti-TCR $\beta$  Ab for stimulation, we performed experiments using peptide Ags presented by APCs. To examine Ag-driven CD4<sup>+</sup> T cell proliferation, lymphocytes from OVA peptide-specific OTII TCR-transgenic or PKC $\theta^{-/-}$  OTII TCR-transgenic mice were purified and stimulated with splenocytes pulsed with a range of concentrations of OVA peptide. As shown in Fig. 2, CD4<sup>+</sup> T cells from PKC $\theta^{-/-}$  OTII mice failed to proliferate in response to all tested concentrations of OVA, whereas OTII CD4<sup>+</sup> T cells showed measurable proliferation at all doses of OVA, particularly at concentrations above 0.2  $\mu$ g/ml. In contrast, an analogous comparison between HY TCR-transgenic and PKC $\theta^{-/-}$  HY TCR-transgenic CD8<sup>+</sup> T cells demonstrated that both HY and PKC $\theta^{-/-}$  HY CD8<sup>+</sup> T cells proliferated in response to all doses of the

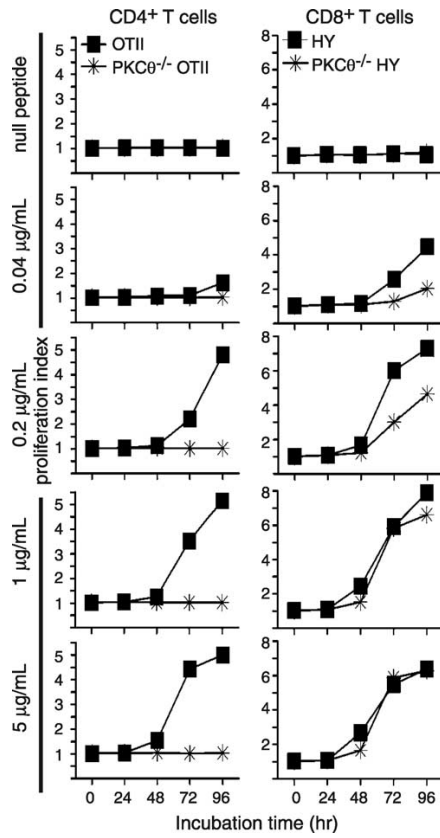


**FIGURE 2.** Defects in  $\text{PKC}\theta^{-/-}$  CD4 $^{+}$  T cell proliferation in response to specific Ag stimulation. CFSE-labeled lymphocytes from the indicated strains of mice were incubated with mitomycin C-inactivated C57BL/6 splenocytes plus the indicated concentrations of stimulatory peptide or 5  $\mu\text{g}/\text{ml}$  of a null variant. Proliferation was assessed at the indicated times by flow cytometry.

stimulatory SMCY peptide. Moreover, at concentrations above 1  $\mu\text{g}/\text{ml}$  SMCY peptide,  $\text{PKC}\theta^{-/-}$  HY CD8 $^{+}$  T cells exhibited WT levels of proliferation (Fig. 2). These results confirm that the proliferative differences between knockout CD4 $^{+}$  and CD8 $^{+}$  T cells are observed upon stimulation with a broad range of concentrations of peptide Ag. These data therefore strongly suggest that the differential proliferative responses of CD4 $^{+}$  and CD8 $^{+}$  T cells from  $\text{PKC}\theta^{-/-}$ ,  $\text{Bcl}10^{-/-}$ , and  $\text{Malt}1^{-/-}$  mice are physiologically relevant.

#### *PKCθ, Bcl10, and Malt1 are required for IL-2 production, but not for expression of CD44 and CD25/IL-2Ra*

Previously published studies demonstrated that  $\text{PKC}\theta^{-/-}$ ,  $\text{Bcl}10^{-/-}$ , and  $\text{Malt}1^{-/-}$  T cells exhibit defective IL-2 production in response to TCR ligation (14–19). However, due to the substantial levels of knockout CD8 $^{+}$  T cell proliferation observed with modest to strong TCR stimuli (Figs. 1 and 2), we felt it was prudent to reexamine IL-2 production by T cells from these knockout animals. Thus, WT,  $\text{PKC}\theta^{-/-}$ , and  $\text{Malt}1^{-/-}$  T cells were stimulated with 100  $\mu\text{g}/\text{ml}$  plate-bound anti-TCR $\beta$ , and supernatants were harvested every 24 h for IL-2 ELISA. As shown in Fig. 3A, WT T cells showed a robust production of IL-2 in response to TCR ligation. In contrast, T cells from  $\text{PKC}\theta^{-/-}$  and  $\text{Malt}1^{-/-}$  mice produced a small amount of IL-2 (2–3 ng/ml) after 48 h of anti-TCR $\beta$  stimulation. IL-2 production by  $\text{Bcl}10^{-/-}$  T cells was

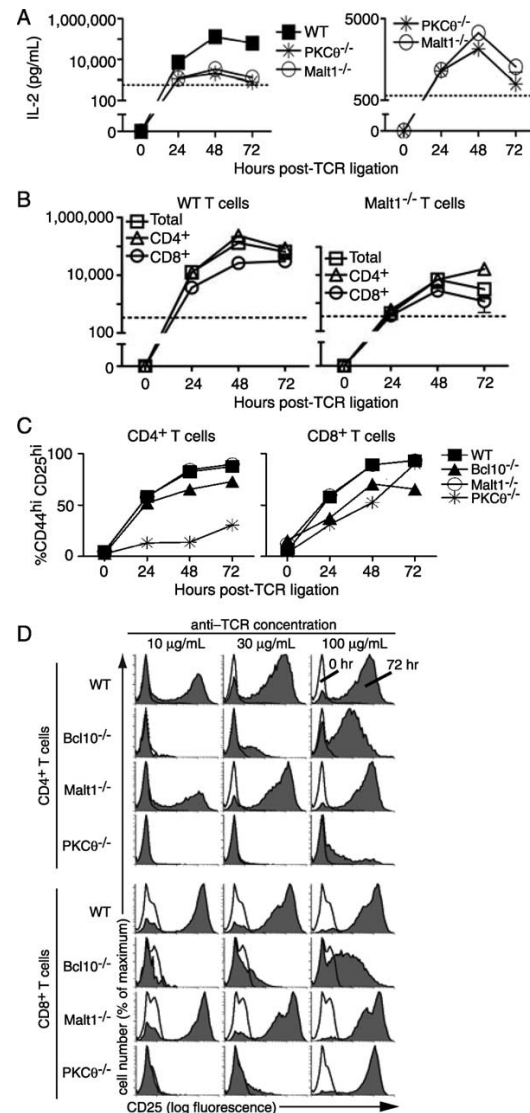


**FIGURE 3.**  $\text{PKC}\theta^{-/-}$ ,  $\text{Bcl}10^{-/-}$ , and  $\text{Malt}1^{-/-}$  T cells show defects in IL-2 production, but up-regulate CD44 and CD25 after TCR ligation. *A*, IL-2 ELISAs of supernatants from cells stimulated with 100  $\mu\text{g}/\text{ml}$  anti-TCR $\beta$  (detection limit = 570 pg/ml). Data are representative of three experiments; bars indicate SEM. *B*, IL-2 ELISAs of total T cells or purified CD4 $^{+}$  or CD8 $^{+}$  T cells from WT or  $\text{Malt}1^{-/-}$  mice stimulated with 100  $\mu\text{g}/\text{ml}$  anti-TCR $\beta$  (detection limit = 340 pg/ml). Data are representative of two biological replicates; bars indicate SEM. *C*, FACS analysis showing the percentage of CD4 $^{+}$  and CD8 $^{+}$  T cells up-regulating both CD44 and CD25 in response to 100  $\mu\text{g}/\text{ml}$  anti-TCR $\beta$ . Data are representative of three experiments at doses ranging from 10 to 100  $\mu\text{g}/\text{ml}$  anti-TCR $\beta$ . *D*, Cells were stimulated with the indicated concentrations of plate-bound anti-TCR $\beta$  and stained every 24 h with Abs to CD25 and CD44. Histogram overlays show CD25 expression on CD4 $^{+}$  and CD8 $^{+}$  T cells at 0 and 72 h after TCR ligation.

generally comparable to that of  $\text{PKC}\theta^{-/-}$  cells (data not shown). The low level of IL-2 secretion by  $\text{Malt}1^{-/-}$  cells is consistent with previously published data (15), although the temporal kinetics of IL-2 production were not reported in that study. Separation of  $\text{Malt}1^{-/-}$  T cells into CD4 $^{+}$  and CD8 $^{+}$  subsets revealed that both CD4 $^{+}$  and CD8 $^{+}$  T cells produce a measurable amount of IL-2,

but CD4<sup>+</sup> T cells made 10× more IL-2 than CD8<sup>+</sup> T cells by 72 h after TCR ligation (Fig. 3B). Similarly, WT CD4<sup>+</sup> T cells produced substantially more IL-2 than WT CD8<sup>+</sup> T cells. Consistent with the results shown in Fig. 3A, WT cells produced much more IL-2 than Malt1<sup>-/-</sup> T cells. Overall, these results indicate that PKCθ<sup>-/-</sup>, Bcl10<sup>-/-</sup>, and Malt1<sup>-/-</sup> T cells are highly deficient in IL-2 production, even under conditions of very strong stimulation through the TCR. Furthermore, assuming that the data from Malt1<sup>-/-</sup> T cells (Fig. 3B) can be generalized, the deficiency in IL-2 production appears to affect CD4<sup>+</sup> and CD8<sup>+</sup> T cells to a similar degree.

In addition to defects in IL-2 production, previous studies of PKCθ<sup>-/-</sup>, Bcl10<sup>-/-</sup>, and Malt1<sup>-/-</sup> T cells have shown impaired up-regulation of cell surface activation markers, particularly CD25. To determine whether the loss of PKCθ, Bcl10, or Malt1 negatively impacts CD44 and CD25 expression under conditions of robust TCR stimulation, T cells were stimulated with anti-TCRβ and the expression of CD44 and CD25 was analyzed over a period of 72 h. As shown in Fig. 3C, CD4<sup>+</sup> T cells from Malt1<sup>-/-</sup> and Bcl10<sup>-/-</sup> mice displayed strong up-regulation of CD44 and CD25 expression after TCR ligation, whereas CD4<sup>+</sup> T cells from PKCθ<sup>-/-</sup> mice increased CD44 and CD25 levels to a lesser extent. Interestingly, CD44 and CD25 expression on all knockout CD8<sup>+</sup> T cells approached WT levels under the highest levels of anti-TCRβ stimulation (100 µg/ml). We also examined the induction of CD25 expression in a dose-response experiment (Fig. 3D). At the two lower doses of anti-TCRβ stimulation (10 and 30 µg/ml), the expression of CD25 on the surface of PKCθ<sup>-/-</sup> and Bcl10<sup>-/-</sup> T cells was reduced compared with WT cells, and the expression of CD25 was only very weakly induced on CD4<sup>+</sup> PKCθ<sup>-/-</sup> T cells at 100 µg/ml anti-TCRβ stimulation. In contrast, the TCR-stimulated expression of CD25 on Malt1<sup>-/-</sup> T cells was slightly reduced at 10 µg/ml anti-TCRβ (Malt1:WT CD25<sup>+</sup> = 39%:49% and 71%:76%, for CD4<sup>+</sup> and CD8<sup>+</sup> T cells, respectively; Fig. 3D and data not shown) and was essentially indistinguishable from WT T cells at the two higher stimulatory doses. These data show that loss of PKCθ, Bcl10, or Malt1 shifts the anti-TCR dose response of CD25 expression (although the loss of Malt1 had only a small impact CD25 expression under the tested conditions). Overall, these results demonstrate that CD44 and CD25 are efficiently up-regulated on CD4<sup>+</sup> and CD8<sup>+</sup> PKCθ<sup>-/-</sup>, Bcl10<sup>-/-</sup>, and Malt1<sup>-/-</sup> T cells, following strong stimulation through the TCR, with the exception of CD4<sup>+</sup> T cells from PKCθ<sup>-/-</sup> mice, which show only a modest up-regulation of these activation markers.

#### *Ectopic IL-2 fails to rescue the proliferative defect of PKCθ<sup>-/-</sup>, Bcl10<sup>-/-</sup>, and Malt1<sup>-/-</sup> CD4<sup>+</sup> T cells*

The TCR-stimulated up-regulation of CD25 on PKCθ<sup>-/-</sup>, Bcl10<sup>-/-</sup>, and Malt1<sup>-/-</sup> T cells suggested that these cells retain the ability to efficiently respond to IL-2, raising the possibility that the proliferative defect of knockout CD4<sup>+</sup> cells could be rescued by ectopic IL-2 under conditions of strong anti-TCR stimulation. To test this hypothesis, T cells were stimulated with anti-TCRβ and cultured with or without rmIL-2. Surprisingly, the addition of IL-2 did not have a substantial impact on the PKCθ<sup>-/-</sup>, Bcl10<sup>-/-</sup>, or Malt1<sup>-/-</sup> CD4<sup>+</sup> T cell proliferation index, regardless of the amount of IL-2 used to supplement the culture (2 or 50 ng/ml; Fig. 4A). In contrast, the addition of IL-2 increased the proliferation index of Bcl10<sup>-/-</sup> CD8<sup>+</sup> T cells to near WT levels by 72 h post-stimulation, while the proliferative index for PKCθ<sup>-/-</sup> CD8<sup>+</sup> T cells exceeded WT levels at 72 h poststimulation. Interestingly, the addition of exogenous IL-2 had little to no effect on the prolifer-

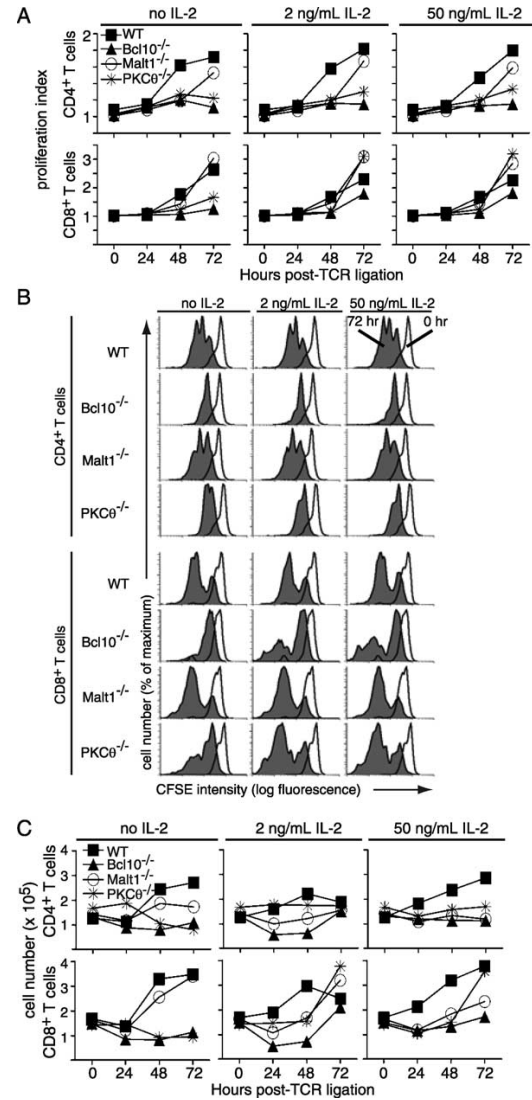


**FIGURE 4.** IL-2 fails to rescue knockout CD4<sup>+</sup> T cell proliferation. **A**, CFSE-labeled T cells were stimulated with 30 µg/ml plate-bound anti-TCRβ and were supplemented with the indicated concentrations of recombinant murine IL-2 at  $t = 24$  h. Proliferation was assessed by FACS at the indicated times poststimulation. **B**, Primary CFSE histogram data from A showing the dilution of CFSE signal in CD4<sup>+</sup> and CD8<sup>+</sup> T cells at 0 and 72 h after TCR ligation. **C**, Total cell number data from A. Cells were counted every 24 h, and live cell numbers were determined by trypan blue staining. Data are representative of two experiments performed with 30–100 µg/ml anti-TCRβ and 1–50 ng/ml rmIL-2.

ation index of Malt1<sup>-/-</sup> CD8<sup>+</sup> T cells. Consistent with these results, the total number of knockout CD4<sup>+</sup> T cells did not increase following the addition of 2 or 50 ng/ml ectopic IL-2, whereas the number of PKCθ<sup>-/-</sup>, Bcl10<sup>-/-</sup>, and Malt1<sup>-/-</sup> CD8<sup>+</sup> T cells increased substantially following the addition of ectopic IL-2 (Fig. 4C). Overall, these data show that ectopic IL-2 does not rescue the proliferative defect of knockout CD4<sup>+</sup> T cells, but does increase the proliferative index and total number of CD8<sup>+</sup> T cells from PKCθ<sup>-/-</sup> and Bcl10<sup>-/-</sup> mice.

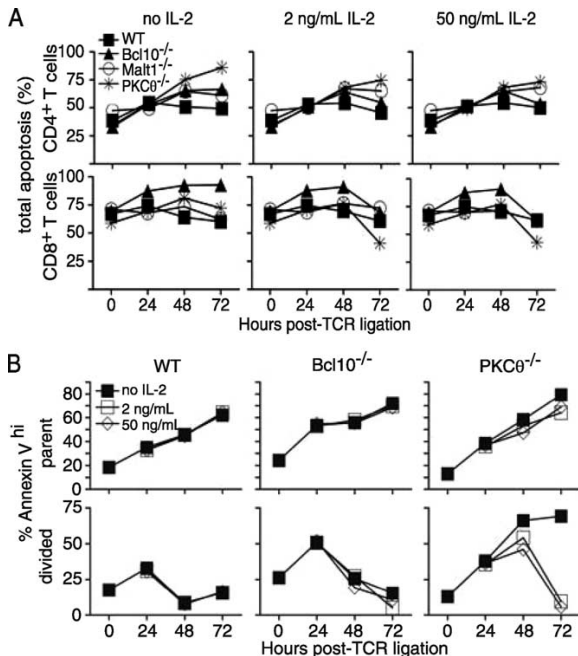


**FIGURE 5.** Ectopic IL-2 improves knockout CD8<sup>+</sup> T cell survival. *A*, T cells from the experiment in 4*A* were stained with anti-CD4 and anti-CD8 Abs and with PI and Hoechst 33342 to measure apoptosis. Data are representative of two experiments performed with 30–100 µg/ml anti-TCR $\beta$  and 1–50 ng/ml rmIL-2. *B*, Quantification of apoptosis in parent (undivided) and divided CD8<sup>+</sup> T cells from WT, PKC $\theta^{-/-}$ , and Bcl10<sup>-/-</sup> mice in the presence or absence of exogenous IL-2. A second experiment using PI to quantify apoptotic cells yielded highly similar results.

#### IL-2 enhances survival of PKC $\theta^{-/-}$ , Bcl10<sup>-/-</sup>, and Malt1<sup>-/-</sup> T cells

The data in Fig. 4*A* demonstrated that ectopic IL-2 has a measurable effect on the proliferative index of CD8<sup>+</sup> T cells from PKC $\theta^{-/-}$  and Bcl10<sup>-/-</sup> mice. However, this effect could be the result of enhanced survival, enhanced proliferation, or both. As shown above (Figs. 1*E* and 4*C*), enumeration of total live cells suggested that proliferating CD8<sup>+</sup> T cells from knockout mice have a survival defect, relative to WT T cells. Close examination of the primary CFSE data showed that the addition of ectopic IL-2 did not appear to increase the number of divisions that WT and knockout CD8<sup>+</sup> T cells undergo, but instead increased the number of divided cells (Fig. 4*B*), suggesting that ectopic IL-2 improved the survival of proliferating cells, but did not promote CD8<sup>+</sup> T cell proliferation. To formally investigate this possibility, we examined the levels of apoptosis in PKC $\theta^{-/-}$ , Bcl10<sup>-/-</sup>, and Malt1<sup>-/-</sup> T cells cultured with and without exogenous IL-2. Cells were harvested every 24 h after plating on anti-TCR $\beta$ -coated wells, and apoptosis was evaluated by staining with PI and Hoechst dyes, identifying cells with loss of membrane integrity and with sub-genomic (<2n) DNA content, respectively. As shown in Fig. 5*A*, knockout CD4<sup>+</sup> and CD8<sup>+</sup> T cells generally exhibited equivalent or higher levels of apoptosis than their WT counterparts at *t* = 0 and at all time points after TCR ligation. However, ectopic IL-2 clearly had a positive effect on PKC $\theta^{-/-}$  and Bcl10<sup>-/-</sup> T cell survival, with PKC $\theta^{-/-}$  CD8<sup>+</sup> T cells showing the greatest reduction in apoptosis at 72 h poststimulation. This effect was maximal at 2 ng/ml, as 50 ng/ml rmIL-2 resulted in the same improvement in knockout T cell survival.

As an additional measure of survival, we directly examined apoptosis in divided and undivided CD8<sup>+</sup> T cells in the presence or absence of ectopic IL-2. Annexin V staining was used to quantify apoptosis in parent and divided cell CD8<sup>+</sup> T cell populations (Fig. 5*B*). This experiment demonstrated that undivided (parent) CD8<sup>+</sup> T cells from WT mice showed higher levels of annexin V staining compared with divided cells. Clearly, the addition of ectopic IL-2 did not appreciably improve the survival of divided or parent WT CD8<sup>+</sup> T cells. In contrast, both undivided and divided CD8<sup>+</sup> T cells from PKC $\theta^{-/-}$  or Bcl10<sup>-/-</sup> mice showed very high levels of annexin V staining, indicating high levels of apoptosis in both populations. The addition of 2 or 50 ng/ml ectopic IL-2 had little effect on the survival of undivided CD8<sup>+</sup> PKC $\theta^{-/-}$  or Bcl10<sup>-/-</sup> T cells, but dramatically improved the survival of divided cells from PKC $\theta^{-/-}$  mice.

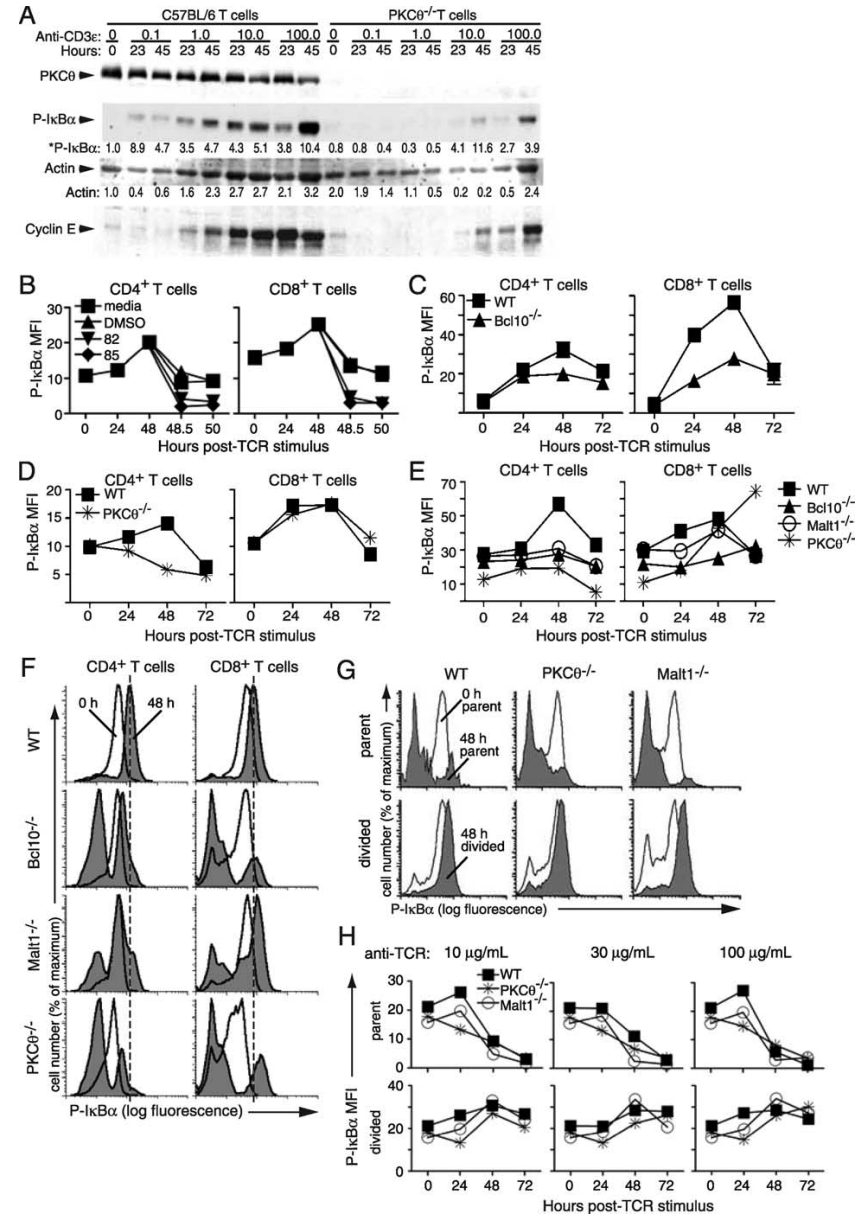
Overall, the data in Figs. 4 and 5 demonstrate that the proliferative defect of PKC $\theta^{-/-}$ , Bcl10<sup>-/-</sup>, and Malt1<sup>-/-</sup> CD4<sup>+</sup> T cells is not the result of defective IL-2 production, since ectopic (or endogenous) IL-2 improved survival, but did not correct the proliferation defect. Thus, an IL-2-independent defect is responsible for the impaired proliferation of PKC $\theta^{-/-}$ , Bcl10<sup>-/-</sup>, and Malt1<sup>-/-</sup> CD4<sup>+</sup> T cells.

#### Residual TCR-mediated phosphorylation of I $\kappa$ B $\alpha$ in CD8<sup>+</sup> T cells from PKC $\theta^{-/-}$ , Bcl10<sup>-/-</sup>, and Malt1<sup>-/-</sup> mice

The above data demonstrated that TCR-stimulated proliferation and up-regulation of activation markers was quite robust in CD8<sup>+</sup> T cells, following modest to high levels of anti-TCR $\beta$  or Ag stimulation. Therefore, either PKC $\theta^{-/-}$ , Bcl10<sup>-/-</sup>, and Malt1<sup>-/-</sup> CD8<sup>+</sup> T cells retain some ability to activate NF- $\kappa$ B, or significant proliferation and up-regulation of activation markers can occur in CD8<sup>+</sup> T cells in the absence of NF- $\kappa$ B activation, under conditions of robust TCR stimulation. To distinguish between these possibilities, we first used Western blotting to examine the kinetics of I $\kappa$ B $\alpha$  phosphorylation (an indicator of IKK activation) in WT vs PKC $\theta^{-/-}$  T cells following TCR ligation. As shown in Fig. 6*A*, WT T cells showed robust activation of NF- $\kappa$ B (indicated by the appearance of phospho-I $\kappa$ B $\alpha$ ) in response to TCR ligation. Additionally, activation of NF- $\kappa$ B correlated well with proliferation, as indicated by expression of cyclin E. In contrast, PKC $\theta^{-/-}$  T cells exhibited greatly reduced NF- $\kappa$ B activation after TCR ligation, with little to no NF- $\kappa$ B activation below 10 µg/ml anti-CD3 $\epsilon$  stimulation. Interestingly, under the strongest conditions of anti-CD3 $\epsilon$  stimulation (10–100 µg/ml), PKC $\theta^{-/-}$  T cells showed clear NF- $\kappa$ B activation and proliferation/cyclin E expression, albeit less than WT cells. These data therefore demonstrated that PKC $\theta^{-/-}$  T cells retain some capacity to activate the IKK complex and proliferate, especially under conditions of strong TCR/CD3 stimulation.

Based on the severe proliferative defect observed in CD4<sup>+</sup> T cells from PKC $\theta^{-/-}$ , Bcl10<sup>-/-</sup>, and Malt1<sup>-/-</sup> mice (Figs. 1 and 2), we hypothesized that CD8<sup>+</sup> T cells accounted for the great majority of I $\kappa$ B $\alpha$  phosphorylation in total T cells from PKC $\theta^{-/-}$  mice (Fig. 6*A*). To rigorously test this hypothesis, we developed a flow cytometry-based assay to detect I $\kappa$ B $\alpha$  phosphorylation in individual CD4<sup>+</sup> and CD8<sup>+</sup> T cells. As shown in Fig. 6*B*, stimulation of WT T cells with plate-bound anti-TCR $\beta$  Ab resulted in an increase in phospho-I $\kappa$ B $\alpha$  in both CD4<sup>+</sup> and CD8<sup>+</sup> T cells over the course of 48 h. To ensure that the increase in phospho-I $\kappa$ B $\alpha$  was due to activity of the IKK complex, we treated cells with the IKK inhibitors BAY11-7082 or BAY11-7085 at 48 h and harvested cells after 30 min and 2 h. As shown in Fig. 6*B*, treatment of CD4<sup>+</sup> and CD8<sup>+</sup> T cells with IKK inhibitors decreased phospho-I $\kappa$ B $\alpha$  fluorescence to nearly

**FIGURE 6.** Differential I $\kappa$ B $\alpha$  phosphorylation in CD4 $^{+}$  and CD8 $^{+}$  T cells from PKC $\theta^{-/-}$ , Bcl10 $^{-/-}$ , and Malt1 $^{-/-}$  mice. *A*, Western blots of whole cell lysates prepared from WT and PKC $\theta^{-/-}$  T cells stimulated with the indicated concentrations of plate-bound anti-CD3 $\epsilon$  plus soluble anti-CD28 (1  $\mu$ g/ml). Data are representative of two experiments. *B*, Validation of the phospho-I $\kappa$ B $\alpha$  flow assay. Purified WT T cells were stimulated with 100  $\mu$ g/ml plate-bound anti-TCR $\beta$  plus 1  $\mu$ g/ml soluble anti-CD28. Media, DMSO, or IKK inhibitors 82 (BAY11-7082) or 85 (BAY11-7085) were added after 48 h, and cells were harvested at 30 min and 2 h. Phospho-I $\kappa$ B $\alpha$  levels were assessed as described in *Materials and Methods*. Data are representative of three experiments. *C–E*, Intracellular FACS analysis of phospho-I $\kappa$ B $\alpha$ . Purified T cells from the indicated strains of mice were stimulated with 100  $\mu$ g/ml plate-bound anti-TCR $\beta$  plus 1  $\mu$ g/ml soluble anti-CD28 (*C*), 100  $\mu$ g/ml plate-bound anti-TCR $\beta$  (*D*), or 30  $\mu$ g/ml plate-bound anti-TCR $\beta$  plus 1  $\mu$ g/ml soluble anti-CD28 (*E*). Error bars in *C*, indicate SD of data from three parallel samples from three mice. Data in *D* are representative of three experiments. Data in *E* are representative of at least three experiments per phenotype performed between 30 and 100 anti-TCR $\beta$ . *F*, Primary histogram data from stimulation experiment in *E* showing 0 (open histograms) and 48 h (gray histograms) after TCR ligation. Dashed line indicates the peak level of I $\kappa$ B $\alpha$  phosphorylation at  $t = 48$  h in WT cells. *G*, Primary histogram overlays showing phospho-I $\kappa$ B $\alpha$  levels in parent and divided CD8 $^{+}$  T cells at  $t = 0$  h (open histograms) and  $t = 48$  h (gray histograms) after TCR ligation. *H*, Quantification of phospho-I $\kappa$ B $\alpha$  levels in parent and divided CD8 $^{+}$  T cells. CFSE labeled cells were stimulated with the indicated concentration of anti-TCR $\beta$ . Parent and divided cells were identified using a similar gating strategy as in Fig. 5*B* and phospho-I $\kappa$ B $\alpha$  levels were determined in each population.



undetectable levels as early as 30 min after the addition of the inhibitor. Although addition of DMSO or medium also resulted in decreased phospho-I $\kappa$ B $\alpha$  levels, presumably due to disturbing T cell interactions with anti-TCR during pipetting, the magnitude of reduction was consistently modest in comparison to cells treated with the IKK inhibitors. The inhibitor data therefore provide strong evidence that the flow cytometry assay specifically detects IKK-dependent phosphorylation of I $\kappa$ B $\alpha$ .

As shown in Fig. 6, *C–E*, TCR stimulation of WT CD4 $^{+}$  T cells leads to a gradual increase in I $\kappa$ B $\alpha$  phosphorylation, with activation levels peaking at 48 h and declining at 72 h after TCR ligation. In contrast, PKC $\theta^{-/-}$ , Bcl10 $^{-/-}$ , and Malt1 $^{-/-}$  CD4 $^{+}$  T cells showed little to no NF- $\kappa$ B activation over the same time period. In the case of CD8 $^{+}$  T cells, the induction of I $\kappa$ B $\alpha$  phosphorylation in WT cells was more rapid, with a significant increase seen by 24 h after TCR $\beta$  stimulation and declining activation by 72 h post-

stimulation. Importantly, PKC $\theta^{-/-}$ , Bcl10 $^{-/-}$ , and Malt1 $^{-/-}$  CD8 $^{+}$  T cells showed clear I $\kappa$ B $\alpha$  phosphorylation, but the kinetics of activation were delayed, with the response peaking at 48 h (Fig. 6, *C* and *D*) or continuing to increase at 72 h (PKC $\theta^{-/-}$  and Bcl10 $^{-/-}$  CD8 $^{+}$  T cells; Fig. 6*E*).

Close examination of the primary flow cytometry data showed that the majority of WT CD4 $^{+}$  and CD8 $^{+}$  T cells phosphorylated I $\kappa$ B $\alpha$  following TCR ligation, as demonstrated by a clear shift in fluorescence intensity 48 h after TCR engagement (Fig. 6*F*). In contrast, CD4 $^{+}$  T cells from knockout animals showed very little I $\kappa$ B $\alpha$  phosphorylation in the same time period, with a subset of cells increasing in fluorescence intensity, but never reaching WT levels. In the case of CD8 $^{+}$  T cells from PKC $\theta^{-/-}$ , Bcl10 $^{-/-}$ , and Malt1 $^{-/-}$  animals, there was also a subset of cells that phosphorylated I $\kappa$ B $\alpha$ , but unlike the CD4 $^{+}$  T cells, the level of activation met or exceeded the levels

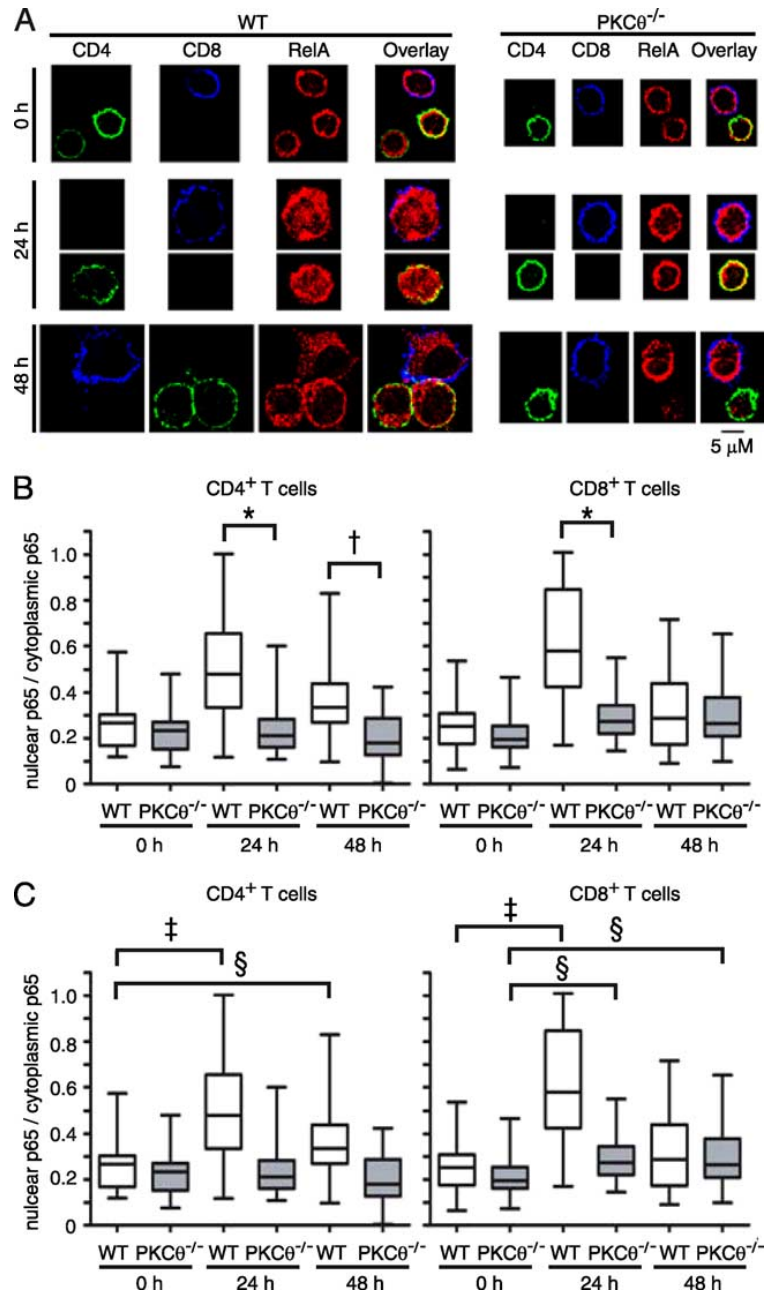


**FIGURE 7.** PKC $\theta^{-/-}$  T cells show defective p65 nuclear localization. *A*, Epifluorescence microscopy images showing nuclear localization of p65 (red) at 0, 24, and 48 h after TCR ligation for WT and PKC $\theta^{-/-}$  CD4 $^{+}$  (green) and CD8 $^{+}$  (blue) cells. *B* and *C*, Quantification of levels of nuclear p65 relative to levels of cytoplasmic p65 at 0, 24, and 48 h after TCR ligation for WT and PKC $\theta^{-/-}$  CD4 $^{+}$  and CD8 $^{+}$  T cells. The box indicates the distribution of values around the median (solid line), while the whiskers indicate the highest and lowest value for each time point. The data analysis strategy is described in detail in *Materials and Methods*. For data analysis, ~30 images were analyzed for each genotype at each time point. Statistical comparisons between WT and PKC $\theta^{-/-}$  and between time points are shown in *B* and *C*, respectively. †,  $p < 0.0001$ ; \*,  $p < 0.0005$ ; ‡,  $p < 0.01$ ; and §,  $p < 0.05$ .

observed in WT cells. In both cell types, a substantial proportion of cells showed little to no I $\kappa$ B $\alpha$  phosphorylation. These results are reminiscent of the proliferation data for knockout CD8 $^{+}$  T cells, in which a proportion of CD8 $^{+}$  T cells from PKC $\theta^{-/-}$ , Bcl10 $^{-/-}$ , and Malt1 $^{-/-}$  mice failed to divide, while a second population proliferated in a manner largely indistinguishable from WT cells, with the exception of a kinetic delay (Fig. 1*D*). Overall, these data strongly suggest that, in response to modest or strong signals through the TCR, the threshold for IKK-stimulated proliferation is met in a subset of PKC $\theta^{-/-}$ , Bcl10 $^{-/-}$ , and Malt1 $^{-/-}$  CD8 $^{+}$  T cells, whereas the threshold required for proliferation is not reached in knockout CD4 $^{+}$  T cells.

To provide further evidence of a mechanistic connection between IKK activity and CD8 $^{+}$  T cell proliferation, we examined phospho-I $\kappa$ B $\alpha$  levels in parent (undivided) and divided populations in response to a range of anti-TCR $\beta$  stimulation. As shown in Fig. 6*G*, there was a clear increase in phospho-I $\kappa$ B $\alpha$  levels in divided cells from WT, PKC $\theta^{-/-}$ , and Malt1 $^{-/-}$  mice after 48 h of stimulation with 100  $\mu$ g/ml anti-TCR $\beta$ . In contrast, parent cells showed a decrease in phospho-I $\kappa$ B $\alpha$  levels, indicating that nonproliferating cells undergo very little NF- $\kappa$ B activation. These data are further quantified in Fig. 6*H*, which shows that in undivided WT cells, phospho-I $\kappa$ B $\alpha$  levels increased from 0 to 24 h following TCR ligation, regardless of the concentration of anti-TCR $\beta$  used to activate the cells. However,

after 24 h, there was a steep decline in phospho-I $\kappa$ B $\alpha$  levels continuing through 72 h. In contrast, divided WT cells showed a steady increase in phospho-I $\kappa$ B $\alpha$  levels over the course of 48 h, followed by a plateau or a slight reduction in phospho-I $\kappa$ B $\alpha$  levels by 72 h. Consistent with and extending the data in Fig. 6*F*, the levels of I $\kappa$ B $\alpha$  phosphorylation in the divided population of both PKC $\theta^{-/-}$  and Malt1 $^{-/-}$  CD8<sup>+</sup> T cells were quite similar to and in some cases exceeded levels seen in WT cells. Overall, these data strongly suggest that those knockout CD8<sup>+</sup> T cells that achieve IKK activation successfully enter the cell cycle, whereas those cells that fail to activate IKK fail to proliferate and eventually apoptose.

To assess NF- $\kappa$ B activation events downstream of I $\kappa$ B $\alpha$  phosphorylation, we used epifluorescence microscopy to directly visualize TCR-stimulated translocation of the p65 (RelA) subunit of NF- $\kappa$ B to the nucleus of WT and PKC $\theta^{-/-}$  T cells. As shown in Fig. 7, *A* and *C*, WT CD4<sup>+</sup> and CD8<sup>+</sup> T cells had little nuclear p65 at  $t = 0$  h, whereas a significant amount of p65 was localized to the nucleus by 24 h. Consistent with the phospho-I $\kappa$ B $\alpha$  data (Fig. 6, *D* and *E*), stimulated PKC $\theta^{-/-}$  CD4<sup>+</sup> T cells showed significantly less nuclear p65 compared with WT CD4<sup>+</sup> T cells at 24 and 48 h after TCR ligation (Fig. 7*B*), and no significant increase in nuclear p65, compared with  $t = 0$  h. Interestingly, PKC $\theta^{-/-}$  CD8<sup>+</sup> T cells showed an increase in p65 over the course of 48 h, with nuclear p65 at 48 h equivalent to WT levels. However, although stimulated PKC $\theta^{-/-}$  CD8<sup>+</sup> T cells displayed increased nuclear p65, the maximal level of p65 nuclear translocation was greatly reduced compared with WT cells, representing a clear difference relative to the I $\kappa$ B $\alpha$  phosphorylation data. Thus, although PKC $\theta^{-/-}$  CD8<sup>+</sup> T cells activate NF- $\kappa$ B, they do so to a lesser extent than WT CD8<sup>+</sup> T cells. Furthermore, the kinetics of p65 nuclear localization differed between the cell types, with peak WT CD8<sup>+</sup> nuclear p65 levels occurring at 24 h, while PKC $\theta^{-/-}$  CD8<sup>+</sup> nuclear p65 levels peaked at 48 h (Fig. 7, *B* and *C*).

Microscopic evaluation of the cells revealed that, overall, PKC $\theta^{-/-}$  T cells remained much smaller than WT T cells after TCR ligation (Fig. 7*A*). However, PKC $\theta^{-/-}$  CD8<sup>+</sup> T cells were larger than PKC $\theta^{-/-}$  CD4<sup>+</sup> T cells at 24 and 48 h, consistent with the p65 translocation data (Fig. 7, *A* and *B*, and data not shown). Moreover, the levels of p65 in many PKC $\theta^{-/-}$  CD4<sup>+</sup> T cells declined substantially by 48 h, relative to PKC $\theta^{-/-}$  CD8<sup>+</sup> T cells and WT T cells (Fig. 7*A*), probably reflecting the high levels of apoptosis in PKC $\theta^{-/-}$  CD4<sup>+</sup> T cells (Fig. 5*A* and data not shown). Overall, these data indicate that PKC $\theta^{-/-}$  CD4<sup>+</sup> T cells undergo little to no p65 nuclear translocation in comparison to WT cells. In contrast, PKC $\theta^{-/-}$  CD8<sup>+</sup> T cells show a reduced level of p65 translocation after TCR ligation, which occurs with delayed kinetics, compared with WT cells. The delayed kinetics of RelA nuclear translocation are consistent with the delayed onset of proliferation (Fig. 1*D*) and the delayed kinetics of I $\kappa$ B $\alpha$  phosphorylation (Fig. 6, *C-E*) observed in PKC $\theta^{-/-}$ , Bcl10 $^{-/-}$ , and Malt1 $^{-/-}$  CD8<sup>+</sup> T cells.

## Discussion

Our data strongly suggest that the proliferative defects of CD4<sup>+</sup> T cells from PKC $\theta^{-/-}$ , Bcl10 $^{-/-}$ , and Malt1 $^{-/-}$  mice are primarily due to a failure to activate NF- $\kappa$ B in response to TCR ligation. In contrast, PKC $\theta^{-/-}$ , Bcl10 $^{-/-}$ , and Malt1 $^{-/-}$  CD8<sup>+</sup> T cells retain some ability to activate NF- $\kappa$ B in response to modest-to-strong TCR stimuli, enabling a proportion of CD8<sup>+</sup> T cells to proliferate. Thus, our data are consistent with a model in which CD8<sup>+</sup> T cells possess a significant alternative NF- $\kappa$ B signaling pathway, which is activated by strong TCR stimula-

tion and which is largely independent of PKC $\theta$ , Bcl10 and Malt1. Although this pathway also appears to exist in CD4<sup>+</sup> T cells, it apparently does not reach the threshold of IKK activation required for significant nuclear translocation of NF- $\kappa$ B p65 and a concomitant proliferative response.

An additional unexpected finding was the observed gradation in the severity of the knockout phenotypes, with Malt1 $^{-/-}$  T cells showing the least impairment with regard to proliferation, IL-2 production, up-regulation of cell surface activation markers, and NF- $\kappa$ B activation. The defects in Bcl10 $^{-/-}$  and PKC $\theta^{-/-}$  T cells were more severe than defects observed in Malt1 $^{-/-}$  T cells, with CD4<sup>+</sup> T cells from PKC $\theta^{-/-}$  mice generally showing the greatest deficits in NF- $\kappa$ B-dependent responses. The heightened severity of the phenotype in PKC $\theta^{-/-}$  T cells may be due to additional TCR signaling defects outside of the NF- $\kappa$ B pathway, particularly impairment of NFAT and AP-1 activation (14, 18, 26). Additionally, the fact that Malt1 $^{-/-}$  T cells have a milder activation deficit than Bcl10 $^{-/-}$  T cells may reflect differences in the NF- $\kappa$ B complexes activated downstream of Bcl10 and Malt1. Specifically, a recent report (27) has shown that, whereas Bcl10 is required for activation of the NF- $\kappa$ B subunits, p65 (RelA) and c-Rel, Malt1 signals lead exclusively to activation of c-Rel. Although those studies examined NF- $\kappa$ B activation in B cells, we believe our data are suggestive that the same or similar signaling differences may also exist in T cells, and that this divergence in TCR activation of p65 and c-Rel may account for the substantial disparity in Bcl10 $^{-/-}$  and Malt1 $^{-/-}$  T cell activation phenotypes. However, further work will be required to show precisely how TCR-stimulated NF- $\kappa$ B activation via Malt1 differs from the NF- $\kappa$ B activation signals that are transduced through PKC $\theta$  and Bcl10.

Similar to previous studies of PKC $\theta^{-/-}$  CD4<sup>+</sup> (28) and CD8<sup>+</sup> (29) T cells, we observed that PKC $\theta$ , Bcl10, and Malt1 are critical factors in T cell survival downstream of TCR signaling. Moreover, each of these proteins appears to play a particularly important role in promoting the survival of actively proliferating CD8<sup>+</sup> T cells. Given that proliferating CD8<sup>+</sup> T cells are rescued from apoptosis by ectopic IL-2 in PKC $\theta^{-/-}$  and Bcl10 $^{-/-}$  mice, our conclusion is that NF- $\kappa$ B-dependent production of IL-2 is a critical mediator of this survival signal. These observations are also important because they demonstrate that NF- $\kappa$ B-dependent TCR-directed proliferative and prosurvival signals are separable, with robust proliferative signals occurring in CD8<sup>+</sup> T cells from PKC $\theta^{-/-}$ , Bcl10 $^{-/-}$ , and Malt1 $^{-/-}$  mice, despite the lack of production of IL-2. The occurrence in PKC $\theta^{-/-}$  mice of productive antiviral CD8<sup>+</sup> T cell immune responses (20) may suggest that, *in vivo*, other survival factors (e.g., IL-7) functionally substitute for IL-2 in rescuing at least some CD8<sup>+</sup> T cells from apoptosis. Given that our data show that IL-2 selectively promotes the survival of dividing PKC $\theta^{-/-}$  CD8<sup>+</sup> T cells, we speculate that, *in vivo*, only those Ag-stimulated cells that successfully enter the proliferative program gain the ability to respond to prosurvival factors such as IL-7.

Previous studies of CD4<sup>+</sup> and CD8<sup>+</sup> proliferation have shown that CD8<sup>+</sup> T cells commit to a proliferative program very rapidly after TCR engagement (1–2 h) (30), while CD4<sup>+</sup> T cells require a much longer duration of TCR signaling (20–24 h) (31, 32). These earlier studies suggested fundamental differences in TCR signaling between CD4<sup>+</sup> and CD8<sup>+</sup> T cells. However, to our knowledge, there have previously been no studies reporting mechanistic differences between CD4<sup>+</sup> and

CD8<sup>+</sup> cells in the TCR-mediated activation of NF- $\kappa$ B signaling. Consequently, our data are important because they establish that there are major differences in how CD4<sup>+</sup> and CD8<sup>+</sup> T cells signal to NF- $\kappa$ B. In addition, our data lend strong support to the hypothesis that NF- $\kappa$ B activation is essential for T cell proliferation. Undivided CD8<sup>+</sup> T cells from WT and knockout mice showed very little IKK activation (I $\kappa$ B $\alpha$  phosphorylation), whereas divided cells showed considerable IKK activity over the course of 72 h (Fig. 6*H*). Furthermore, divided knockout T cells showed WT levels of phospho-I $\kappa$ B $\alpha$ , indicating that those knockout T cells that proliferated also activated the IKK complex to a similar extent as WT T cells.

Direct visualization of the p65 subunit of NF- $\kappa$ B revealed a surprising discordance between I $\kappa$ B $\alpha$  phosphorylation and p65 translocation. Specifically, levels of nuclear p65 substantially decreased from 24 to 48 h after TCR ligation in WT CD8<sup>+</sup> T cells, while phospho-I $\kappa$ B $\alpha$  levels peaked in WT CD8<sup>+</sup> T cells at 48 h. These two seemingly contradictory pieces of data suggest that other mechanisms of controlling p65 nuclear localization are at work at later time points and/or after prolonged stimulation through the TCR (in WT cells). Indeed, kinetic analysis of the NF- $\kappa$ B pathway previously revealed that I $\kappa$ B $\alpha$  plays a dominant role in controlling the NF- $\kappa$ B response early after stimulation, whereas I $\kappa$ B $\beta$  and I $\kappa$ B $\epsilon$  are involved in controlling later responses (33). These findings suggest that the nuclear localization of p65 is controlled by I $\kappa$ B $\alpha$  at early points after TCR ligation, while I $\kappa$ B $\beta$  and I $\kappa$ B $\epsilon$  may play a more dominant regulatory role at later points.

Another NF- $\kappa$ B regulatory mechanism that may be relevant to our observations is that, at later time points, the rate of p65 nuclear export exceeds the rate of p65 nuclear import. It has been shown that p65 is acetylated after nuclear localization, which reduces its binding affinity for DNA and enhances nuclear export by I $\kappa$ B $\alpha$  (34). Furthermore, the nuclear localization rate of I $\kappa$ B $\alpha$  exceeds the nuclear localization rate of p65 (35). The combination of p65 acetylation and rapid I $\kappa$ B $\alpha$  shuttling to the nucleus may result in a net decrease of nuclear p65 at later time points (48 h) after TCR ligation.

Either or both of the above mechanisms may limit the amount of p65 that can accumulate in the nucleus at late time points (48 h and beyond) after TCR stimulation, regardless of the level of IKK activity. Such mechanisms may explain why PKC $\theta^{-/-}$  CD8<sup>+</sup> T cells (and presumably Bcl10 $^{-/-}$  and Malt1 $^{-/-}$  CD8<sup>+</sup> T cells) fail to accumulate nuclear p65 to the degree seen in WT T cells at 24 h, despite the high levels of phospho-I $\kappa$ B $\alpha$  observed in PKC $\theta^{-/-}$  CD8<sup>+</sup> T cells by 48 h. Although previous work has shown that NF- $\kappa$ B responses are proportional to the duration of stimulus for at least 6 h (33), our data and the above-cited studies strongly suggest that there are potent homeostatic mechanisms that limit terminal NF- $\kappa$ B activation steps in T cells (i.e., p65 nuclear translocation) at late time points (by 48 h), despite continued TCR engagement and IKK activation.

Overall, our data suggest an interesting dichotomy in the way that CD4<sup>+</sup> and CD8<sup>+</sup> T cells signal to NF- $\kappa$ B. Further work will be required to determine the precise molecular mechanisms that allow CD8<sup>+</sup> T cells to successfully activate NF- $\kappa$ B and divide in the absence of PKC $\theta$ , Bcl10, or Malt1.

## Acknowledgments

We thank A. Kupfer and D. Littman for PKC $\theta^{-/-}$  mice, T. Mak for Bcl10 $^{-/-}$  and Malt1 $^{-/-}$  mice, S. Maynard for care and screening of mice, and A. Kashyap for general technical support. We also thank C. Olsen for help with statistical analyses, C.-Z. Giam, and P. Love for critical review

of this work, and F. Crawford and J. Kappler for providing the MKASSAY program.

## Disclosures

The authors have no financial conflict of interest.

## References

1. Hayden, M. S., and S. Ghosh. 2004. Signaling to NF- $\kappa$ B. *Genes Dev.* 18: 2195–2224.
2. Li, Q., and I. M. Verma. 2002. NF- $\kappa$ B regulation in the immune system. *Nat. Rev. Immunol.* 2: 725–734.
3. Schulze-Luehrmann, J., and S. Ghosh. 2006. Antigen-receptor signaling to nuclear factor  $\kappa$ B. *Immunity* 25: 701–715.
4. Matsumoto, R., D. Wang, M. Blonska, H. Li, M. Kobayashi, B. Pappu, Y. Chen, D. Wang, and X. Lin. 2005. Phosphorylation of CARMA1 plays a critical role in T cell receptor-mediated NF- $\kappa$ B activation. *Immunity* 23: 575–585.
5. Sommer, K., B. Guo, J. L. Pomerantz, A. D. Bandaranayake, M. E. Moreno-Garcia, Y. L. Ovechkin, and D. J. Rawlings. 2005. Phosphorylation of the CARMA1 linker controls NF- $\kappa$ B activation. *Immunity* 23: 561–574.
6. Che, T., Y. You, D. Wang, M. J. Tanner, V. M. Dixit, and X. Lin. 2004. MALT1/paracaspase is a signaling component downstream of CARMA1 and mediates T cell receptor-induced NF- $\kappa$ B activation. *J. Biol. Chem.* 279: 15870–15876.
7. Gaide, O., B. Favier, D. F. Legler, D. Bonnet, B. Brissoni, S. Valitutti, C. Bron, J. Tschopp, and M. Thome. 2002. CARMA1 is a critical lipid raft-associated regulator of TCR-induced NF- $\kappa$ B activation. *Nat. Immunol.* 3: 836–843.
8. McAllister-Lucas, L. M., N. Inohara, P. C. Lucas, J. Ruland, A. Benito, Q. Li, S. Chen, F. F. Chen, S. Yamaoka, I. M. Verma, et al. 2001. Bimp1, a MAGUK family member linking protein kinase C activation to Bcl10-mediated NF- $\kappa$ B induction. *J. Biol. Chem.* 276: 30589–30597.
9. Sun, L., L. Deng, C. K. Ea, Z. P. Xia, and Z. J. Chen. 2004. The TRAF6 ubiquitin ligase and TAK1 kinase mediate IKK activation by BCL10 and MALT1 in T lymphocytes. *Mol. Cell* 14: 289–301.
10. Zhou, H., M. Q. Du, and V. M. Dixit. 2005. Constitutive NF- $\kappa$ B activation by the t(11;18)(q21;q21) product in MALT lymphoma is linked to deregulated ubiquitin ligase activity. *Cancer Cell* 7: 425–431.
11. Su, H., N. Bidere, L. Zheng, A. Cubre, K. Sakai, J. Dale, L. Salmena, R. Hakem, S. Straus, and M. Lenardo. 2005. Requirement for caspase-8 in NF- $\kappa$ B activation by antigen receptor. *Science* 307: 1465–1468.
12. Misra, R. S., J. Q. Russell, A. Koenig, J. A. Hinshaw-Makepeace, R. Wen, D. Wang, H. Huo, D. R. Littman, U. Ferch, J. Ruland, et al. 2007. Caspase-8 and c-FLIPL associate in lipid rafts with NF- $\kappa$ B adaptors during T cell activation. *J. Biol. Chem.* 282: 19365–19374.
13. Karin, M., and Y. Ben-Neriah. 2000. Phosphorylation meets ubiquitination: the control of NF- $\kappa$ B activity. *Annu. Rev. Immunol.* 18: 621–663.
14. Pfeifferhofer, C., K. Kofer, T. Gruber, N. G. Tabrizi, C. Lutz, K. Maly, M. Leitges, and G. Baier. 2003. Protein kinase C  $\theta$  affects Ca $^{2+}$  mobilization and NFAT cell activation in primary mouse T cells. *J. Exp. Med.* 197: 1525–1535.
15. Rueffli-Brasse, A. A., D. M. French, and V. M. Dixit. 2003. Regulation of NF- $\kappa$ B-dependent lymphocyte activation and development by paracaspase. *Science* 302: 1581–1584.
16. Ruland, J., G. S. Duncan, A. Elia, I. del Barco Barrantes, L. Nguyen, S. Plyte, D. G. Millar, D. Bouchard, A. Wakeham, P. S. Ohashi, and T. W. Mak. 2001. Bcl10 is a positive regulator of antigen receptor-induced activation of NF- $\kappa$ B and neural tube closure. *Cell* 104: 33–42.
17. Ruland, J., G. S. Duncan, A. Wakeham, and T. W. Mak. 2003. Differential requirement for Malt1 in T and B cell antigen receptor signaling. *Immunity* 19: 749–758.
18. Sun, Z., C. W. Arendt, W. Ellmeier, E. M. Schaeffer, M. J. Sunshine, L. Gandhi, J. Annes, D. Petrzilka, A. Kupfer, P. L. Schwartzberg, and D. R. Littman. 2000. PKC- $\theta$  is required for TCR-induced NF- $\kappa$ B activation in mature but not immature T lymphocytes. *Nature* 404: 402–407.
19. Xue, L., S. W. Morris, C. Orihuela, E. Tuomanen, X. Cui, R. Wen, and D. Wang. 2003. Defective development and function of Bcl10-deficient follicular, marginal zone and B1 B cells. *Nat. Immunol.* 4: 857–865.
20. Marsland, B. J., C. Nembrini, N. Schmitz, B. Abel, S. Krautwald, M. F. Bachmann, and M. Kopf. 2005. Innate signals compensate for the absence of PKC- $\theta$  during in vivo CD8<sup>+</sup> T cell effector and memory responses. *Proc. Natl. Acad. Sci. USA* 102: 14374–14379.
21. Barnden, M. J., J. Allison, W. R. Heath, and F. R. Carbone. 1998. Defective TCR expression in transgenic mice constructed using cDNA-based  $\alpha$ - and  $\beta$ -chain genes under the control of heterologous regulatory elements. *Immunol. Cell Biol.* 76: 34–40.
22. Kisielow, P., H. Bluthmann, U. D. Staerz, M. Steinmetz, and H. von Boehmer. 1988. Tolerance in T-cell-receptor transgenic mice involves deletion of nonnative CD4 $^{+}$  thymocytes. *Nature* 333: 742–746.
23. Robertson, J. M., P. E. Jensen, and B. D. Evavold. 2000. DO11.10 and OT-II T cells recognize a C-terminal ovalbumin 323–339 epitope. *J. Immunol.* 164: 4706–4712.
24. Santori, F. R., K. Holmberg, D. Ostrov, N. R. Gascoigne, and S. Vukmanovic. 2004. Distinct footprints of TCR engagement with highly homologous ligands. *J. Immunol.* 172: 7466–7475.
25. Schaefer, B. C., J. W. Kappler, A. Kupfer, and P. Marrack. 2004. Complex and dynamic redistribution of NF- $\kappa$ B signaling intermediates in response to T cell receptor stimulation. *Proc. Natl. Acad. Sci. USA* 101: 1004–1009.

26. Manicassamy, S., M. Sadim, R. D. Ye, and Z. Sun. 2006. Differential roles of PKC-θ in the regulation of intracellular calcium concentration in primary T cells. *J. Mol. Biol.* 355: 347–359.
27. Ferch, U., C. M. zum Buschenfelde, A. Gewies, E. Wegener, S. Rauser, C. Peschel, D. Krappmann, and J. Ruland. 2007. MALT1 directs B cell receptor-induced canonical nuclear factor-κB signaling selectively to the c-Rel subunit. *Nat. Immunol.* 8: 984–991.
28. Manicassamy, S., S. Gupta, Z. Huang, and Z. Sun. 2006. Protein kinase C-θ-mediated signals enhance CD4<sup>+</sup> T cell survival by up-regulating Bcl-x<sub>L</sub>. *J. Immunol.* 176: 6709–6716.
29. Barouch-Bentov, R., E. E. Lemmens, J. Hu, E. M. Janssen, N. M. Droin, J. Song, S. P. Schoenberger, and A. Altman. 2005. Protein kinase C-θ is an early survival factor required for differentiation of effector CD8<sup>+</sup> T cells. *J. Immunol.* 175: 5126–5134.
30. van Stipdonk, M. J., E. E. Lemmens, and S. P. Schoenberger. 2001. Naive CTLs require a single brief period of antigenic stimulation for clonal expansion and differentiation. *Nat. Immunol.* 2: 423–429.
31. Iezzi, G., K. Karjalainen, and A. Lanzavecchia. 1998. The duration of antigenic stimulation determines the fate of naive and effector T cells. *Immunity* 8: 89–95.
32. Jelley-Gibbs, D. M., N. M. Lepak, M. Yen, and S. L. Swain. 2000. Two distinct stages in the transition from naive CD4 T cells to effectors, early antigen-dependent and late cytokine-driven expansion and differentiation. *J. Immunol.* 165: 5017–5026.
33. Hoffmann, A., A. Levchenko, M. L. Scott, and D. Baltimore. 2002. The IκB-NF-κB signaling module: temporal control and selective gene activation. *Science* 298: 1241–1245.
34. Kiernan, R., V. Bres, R. W. Ng, M. P. Coudart, S. El Messaoudi, C. Sardet, D. Y. Jin, S. Emiliani, and M. Benkirane. 2003. Post-activation turn-off of NF-κB-dependent transcription is regulated by acetylation of p65. *J. Biol. Chem.* 278: 2758–2766.
35. Birbach, A., P. Gold, B. R. Binder, E. Hofer, R. de Martin, and J. A. Schmid. 2002. Signaling molecules of the NF-κB pathway shuttle constitutively between cytoplasm and nucleus. *J. Biol. Chem.* 277: 10842–10851.

**Chapter 3: The terminal events in TCR-mediated activation of NF- $\kappa$ B are digital.**

**Lara M. Kingeter and Brian C. Schaefer**

*A Cutting Edge Manuscript for submission to the Journal of Immunology*

## **Abstract**

T cell receptor (TCR) mediated activation of the transcription factor NF- $\kappa$ B is a key event in T cell activation and gain of effector function. While most of the proteins involved in this signal transduction pathway have been identified, it is not known if TCR signaling to NF- $\kappa$ B is digital (switch-like) or analog (graded) in nature. We have examined the terminal steps in this signaling cascade, and found that the phosphorylation of both I $\kappa$ B $\alpha$  and the NF- $\kappa$ B subunit p65 is digital, as the intensity of the phosphorylation signal was consistent and not affected by increasing anti-TCR $\beta$  concentrations. Furthermore, stimulating T cells with increasing concentrations of anti-TCR $\beta$  had a positive effect on the number of responding cells, indicating that under these conditions, stronger TCR signals do not affect the NF- $\kappa$ B response of individual cells, but serve to increase the number of responding cells. We discuss two distinct models to account for these signaling characteristics in T cells.

## **Introduction**

NF- $\kappa$ B is a transcription factor of central importance in T cell biology, controlling the expression of genes involved in proliferation, gain of effector function, and survival (reviewed in (1)). The NF- $\kappa$ B family of transcription factors consists of 5 structurally similar proteins: RelA (p65), RelB, cRel, p100/p52, and p105/p50. The NF- $\kappa$ B proteins form homo-or heterodimers via Rel-homology domain interactions; traditionally, ‘NF- $\kappa$ B’ refers to the p65:p50 heterodimer.

Many of the proteins involved in T cell receptor (TCR)-mediated activation of NF- $\kappa$ B have been identified and characterized. Briefly, following TCR engagement by cognate peptide displayed in the context of an MHC molecule, the protein tyrosine kinase Lck phosphorylates tyrosine residues in the ITAM regions of the TCR complex. This phosphorylation leads to the recruitment and activation of adaptor proteins and kinases, including Zap70, LAT, SLP-76, PLC- $\gamma$ 1, and PKC $\theta$ . These proteins transduce activating signals to the CBM complex, a protein complex consisting of the membrane guanylate kinase Carma1, the adaptor protein Bcl10, and the paracaspase Malt1. The CBM complex serves to nucleate the ubiquitin ligase TRAF6, activating TRAF6 and allowing it to ubiquitinate and activate the IKK complex. The IKK complex then phosphorylates I $\kappa$ B $\alpha$ , an inhibitor protein that retains the NF- $\kappa$ B dimer in the cytoplasm by masking its nuclear localization sequences. I $\kappa$ B $\alpha$  phosphorylation triggers its ubiquitination and subsequent

proteasomal degradation, freeing NF-κB to enter the nucleus. Once in the nucleus, the p65 subunit of NF-κB is phosphorylated, a modification which enhances the ability of p65 to recruit transcriptional machinery and control the expression of target genes (reviewed in (2)).

Although most of the key players in NF-κB signal transduction are known, it is unclear if TCR signaling to NF-κB is digital or analog in nature. Digital signaling is switch-like, and is either ‘on or off’ with no intermediate state. In digital signaling, once the threshold for signaling has been met, the intensity of the output signal is constant and is not dependent on the intensity of the input stimulus. In contrast, analog signaling is graded in nature, with the intensity of the output signal proportional to the intensity of the input stimulus. The simplest example of analog signaling is a dose response curve. While natural systems never behave as absolutes, certain pathways are more digital in nature, while others are more analog. Frequently, signal transduction pathways combine digital and analog features to achieve exquisite control over biological outcomes. An example of this is Erk signaling in T cells. A recent report identified Erk phosphorylation in T cells as being digital, while the inhibitor SHP-1 behaves in an analog fashion (3). This model predicts signals generated from weak TCR ligands will not be strong enough to overcome SHP-1 inhibition, and therefore will not trigger the digital phosphorylation of Erk. In contrast, strong TCR ligands will quickly overcome the analog nature of SHP-1 inhibition and will trigger Erk phosphorylation and T cell activation (4, 3).

Another example of combinatorial signaling is the Ras pathway ((5) and reviewed in (6)). Plasma membrane Ras nanoclusters activate Erk in a digital manner, but the

number of signaling Ras nanoclusters is dependent on the strength of the input signal (EGF concentration). In this way, the number of “on” Ras nanoclusters tunes the magnitude of the output response, allowing the cell to appropriately respond to different concentrations of stimuli.

Given the importance of NF- $\kappa$ B in T cell function, characterizing the digital or analog nature of NF- $\kappa$ B signaling will enhance our understanding of how T cells regulate signal transduction pathways following TCR ligation. We utilized a series of *in vitro* dose-response and phosphorylation experiments to characterize the nature of TCR-mediated signaling to NF- $\kappa$ B, and found that the terminal activation events are digital in nature. The intensity of I $\kappa$ B $\alpha$  and p65 phosphorylation is relatively constant, regardless of the concentration of anti-TCR $\beta$  antibody used to stimulate the cells. Interestingly, as the anti-TCR $\beta$  concentration increases, the number of cells in the response peak increases. These results suggest that the strength of TCR stimulation does not affect the magnitude of the signaling response, but instead triggers the activation of a greater number of cells, resulting in a stronger T cell response. We propose and discuss two distinct models to account for these signaling characteristics.

## **Methods**

### *Mice*

C57BL/6 (WT) mice, 4-8 weeks old, were purchased from NCI (Frederick, MD). OTII mice (7) between 6-10 weeks old were bred in-house, following crossing to C57BL/6 for more than 10 generations. All experiments were approved by the USUHS IACUC.

### *T cell stimulation*

Lymph nodes were harvested from mice and placed in ice cold EHAA media. Lymph nodes were physically disrupted and passed through a 70  $\mu\text{m}$  filter to generate a single-cell suspension. In one experiment (Fig. 1) T cells were purified as previously described (8). Lymphocytes were rested overnight at 37° C + 5% CO<sub>2</sub> (Fig. 1), plated immediately (Fig. 2), or rested on ice for 3 hours (Fig. 3). In Fig. 1 and Fig. 3, 4-4.5 x 10<sup>5</sup> lymphocytes/well were plated in a 96-well plate coated with the indicated concentrations of anti-TCR $\beta$  (H597) antibody. OTII stimulation was performed as previously described (8).

### *Intracellular staining*

Following 48 h of stimulation, cells were harvested and fixed with 2%

paraformaldehyde, followed by surface marker staining with anti-CD8 PerCP (53-6.7; BD Pharmingen) and anti-CD4 PE (GK1.5; eBioscience). Cells were washed twice, permeabilized, and stained overnight with either rabbit monoclonal antibody to phospho-I $\kappa$ B $\alpha$  (Ser32, Cell Signaling Technology) or rabbit monoclonal antibody to phospho-p65 (Ser 536; 93H1, Cell Signaling Technology), followed by incubation with goat anti-rabbit Alexa 647 (Invitrogen) or goat anti-rabbit Alexa 488 (Molecular Probes).

*Flow cytometry*

Flow cytometry was performed on a Beckman-Coulter LSRII, and data analysis was performed using WinList 5.0.

## **Results and Discussion**

### **TCR ligation leads to digital I $\kappa$ B $\alpha$ phosphorylation**

Previously, we developed and validated a flow cytometry based assay that permits the specific detection of phospho-I $\kappa$ B $\alpha$  in CD4 $^{+}$  and CD8 $^{+}$  T cells (8). Using this method, we examined the phosphorylation of I $\kappa$ B $\alpha$  in WT T cells in response to *in vitro* stimulation with a range of anti-TCR $\beta$  concentrations. T cells were stimulated with the indicated concentrations of anti-TCR $\beta$ , and cells were harvested every 24 hours and phospho-I $\kappa$ B $\alpha$  levels examined. We found that phospho-I $\kappa$ B $\alpha$  levels peak after 48 hours of stimulation (data not shown and (8)), so we chose to further investigate the characteristics of I $\kappa$ B $\alpha$  phosphorylation at this time point. As shown in Figure 1A, T cells stimulated with very low concentrations (0.032-0.8  $\mu$ g/mL) of anti-TCR $\beta$  did not increase I $\kappa$ B $\alpha$  phosphorylation above baseline levels (not shown). However, stimulation with 4  $\mu$ g/mL anti-TCR $\beta$  resulted in the appearance of a small activation peak, and this peak was maintained and increased in size following stimulation with higher concentrations of anti-

TCR $\beta$  (20 and 100  $\mu\text{g/mL}$ ). The intensity of the activation peak was relatively constant, and quantification of the mean fluorescence intensity of the activation peaks confirm that peak intensity did not change considerably as the concentration of anti-TCR $\beta$  stimulation increased (Fig. 1B).

While the magnitude of the input stimulus (anti-TCR $\beta$  concentration) did not appear to affect the output signal intensity (phospho-I $\kappa$ B $\alpha$  levels), the concentration of anti-TCR $\beta$  did augment the number of responding cells, with the percentage of CD4 $^+$  and CD8 $^+$  T cells in the activation peak increasing in response to stimulation with higher anti-TCR $\beta$  concentrations (Fig. 1C). These data suggest that under these conditions, once the threshold for signaling has been met, the strength of TCR stimulation does not affect the magnitude of the response of individual cells, but instead acts to increase the number of activated cells in the overall population. However, it is important to note that even at the highest stimulatory concentration (100  $\mu\text{g/mL}$  anti-TCR $\beta$ ) there is still a population of non-responding cells (Fig. 1A and Fig. 1C). It is possible that these ‘non-responders’ could be recruited to the activation peak provided a high enough concentration of anti-TCR antibody stimulation. Conversely, these non-responding cells may represent a dying or otherwise impaired portion of the T cell population that is not capable of responding under any stimulation conditions.

**Figure 1. TCR-mediated phosphorylation of I $\kappa$ B $\alpha$  is digital.** A) Primary histograms showing phospho-I $\kappa$ B $\alpha$  intensity following 48 hours of stimulation with the indicated concentrations of plate-bound anti-TCR $\beta$ . The dashed line shows peak overlays. B) Adjusted MFI values of phospho-I $\kappa$ B $\alpha$  peak (MFI of activation peak – MFI of control peak (not shown)). C) Percent of T cells in the activation peak. Data are representative of 3 experiments conducted with a range of anti-TCR $\beta$  concentrations.

Overall, the data in Figure 1 demonstrate that I $\kappa$ B $\alpha$  phosphorylation following TCR ligation is a digital event, and that increasing the strength of TCR stimulation has little effect on the response of individual cells, but rather serves to increase the number of responding cells.

### **Digital I $\kappa$ B $\alpha$ phosphorylation is antigen specific**

We next sought to evaluate if I $\kappa$ B $\alpha$  is phosphorylated in a digital manner following TCR interaction with cognate antigen presented by an antigen presenting cell. OTII CD4 $^{+}$  T cells express a transgenic TCR specific for a peptide fragment from chicken ovalbumin (pOVA); we examined antigen-specific I $\kappa$ B $\alpha$  phosphorylation by incubating OTII lymphocytes with pOVA-pulsed splenocytes. As shown in Figure 2A, stimulation of OTII T cells with the null pOVA variant (331K) or very low concentrations of stimulatory pOVA (0.04  $\mu$ g/mL) did not result in I $\kappa$ B $\alpha$  phosphorylation above baseline levels (not shown). However, a pOVA concentration as low as 0.2  $\mu$ g/mL did result in the appearance of a phospho-I $\kappa$ B $\alpha$  activation peak. Reminiscent of the data in Figure 1, the intensity of the activation peak did not change with increasing pOVA concentrations (Fig. 2A and B), but the percentage of cells in the activation peak did increase (Fig. 2C). Again, even at the highest concentration of pOVA (5  $\mu$ g/mL), a portion of the antigen-specific T cell population was not activated, indicating that the non-responsive population seen in Figure 1 was not an artifact of anti-TCR $\beta$  stimulation.

**Figure 2. Digital I $\kappa$ B $\alpha$  phosphorylation in response to peptide antigen stimulation.** OTII T cells were stimulated with the indicated concentrations of pOVA, and I $\kappa$ B $\alpha$  phosphorylation evaluated after 48 hours. A) Primary histograms showing phospho-I $\kappa$ B $\alpha$  levels at 48 hours; the dashed line shows peak overlays. B) Adjusted MFI values of phospho-I $\kappa$ B $\alpha$  peak (MFI of activation peak – MFI of control peak (not shown)). C) Percentage of OTII T cells in the activation peak. Data are representative of one experiment.

Taken together, the data in Figure 2 confirm that TCR-mediated I $\kappa$ B $\alpha$  phosphorylation is digital, and occurs in an antigen-specific manner.

### p65 phosphorylation is digital

The digital nature of I $\kappa$ B $\alpha$  phosphorylation led us to speculate that the terminal events in NF- $\kappa$ B activation are digital as well. One of these events is the phosphorylation of the NF- $\kappa$ B subunit p65, a modification that enhances the ability of p65 to recruit transcriptional machinery (2). Using our FACS-based assay, we examined p65 phosphorylation following TCR ligation. As shown in Figure 3A, stimulation with very low concentrations of anti-TCR $\beta$  did not result in the appearance of a phospho-p65 peak. However, reminiscent of the phospho-I $\kappa$ B $\alpha$  data, stimulation with 4 mg/mL anti-TCR $\beta$  did result in the appearance of a small activation peak. As with phospho-I $\kappa$ B $\alpha$ , the intensity of the phospho-p65 peak did not change as the anti-TCR $\beta$  concentration was increased (Fig. 3A and B).

**Figure 3. p65 phosphorylation is digital.** A) Primary histograms showing phospho-p65 intensity following 48 hours of stimulation with the indicated concentrations of plate-bound anti-TCR $\beta$ . The dashed line shows peak overlays. B) Adjusted MFI values of phospho-p65 peak (MFI of activation peak – MFI of control peak (not shown)). C) Percent of T cells in the activation peak. Data are representative of 3 experiments conducted with a range of anti-TCR $\beta$  concentrations.

As shown in Figure 3C, the percentage of cells in the activation peak showed a positive correlation with anti-TCR $\beta$  concentration. Consistent with the results in Figures 1

and 2, a portion of the T cell population remains unresponsive even at the highest doses of anti-TCR $\beta$  stimulation.

Overall, these data support the conclusion that the terminal events in TCR signaling to NF- $\kappa$ B are digital. The practical consequence of this finding is that once the threshold for signaling has been met, I $\kappa$ B $\alpha$  and p65 phosphorylation will occur in a switch-like, on-off fashion. While these results are intriguing, a major unresolved question concerns the behavior of upstream proteins; in particular, at what point does this signal become digital? There are 2 potential models to address this question. One possibility is that the digitization of the signal occurs very early in the pathway, at the level of the TCR complex at the membrane (Fig. 4A). Ras nanoclusters provide a relevant example of proteins in the plasma membrane digitizing an analog signal (6). This model predicts that after TCR engagement, signals from the TCR complex are propagated in a digital manner, with each downstream protein or protein complex being turned ‘on’ to transduce the signal; in other words, a ‘chain-reaction’ of signaling. While this model is a formal possibility, it is unlikely that the many diverse proteins involved in TCR-to-NF- $\kappa$ B signal transduction all function in a digital, ‘on or off’ manner. Therefore, it is unlikely that signaling to NF- $\kappa$ B is digitized at the level of the TCR complex.

**Figure 4. Two models of NF- $\kappa$ B signaling.** In panel A, TCR engagement results in a digital signal to NF- $\kappa$ B, with little opportunity for the T cell to control downstream signaling events after TCR engagement. In panel B, membrane proximal signaling events post-TCR ligation leads to the activation of the IKK complex, which in turn, propagates the signal to NF- $\kappa$ B in a digital manner.

A second possibility is that a downstream protein complex (such as the IKK complex) acts to convert analog signals (such as phosphorylation and activation of

upstream proteins) to a digital signal (Fig. 4B). This model suggests that membrane-proximal signaling events converge to overcome the ‘activation energy’ of the enzymatically active IKK complex. Upon activation, the IKK complex then digitally phosphorylates the  $I\kappa B\alpha$  protein, and the resulting downstream events are initiated. This model better accounts for T cell non-responsiveness to self-ligand or weakly binding ligands, because by digitizing the signal at a later point in the pathway, T cells can achieve a greater degree of control over signaling events and prevent the inappropriate activation of this important transcription factor.

Taken together, these results will serve to stimulate interest in a poorly investigated aspect of T cell biology, and specifically, will inform investigations into additional characteristics of T cell signaling to NF- $\kappa$ B.

### References

1. Hayden, M. S., and S. Ghosh. 2004. Signaling to NF-kappaB. *Genes Dev* 18:2195-2224.
2. Vermeulen, L., G. De Wilde, S. Notebaert, W. Vanden Berghe, and G. Haegeman. 2002. Regulation of the transcriptional activity of the nuclear factor-kappaB p65 subunit. *Biochem Pharmacol* 64:963-970.
3. Altan-Bonnet, G., and R. N. Germain. 2005. Modeling T cell antigen discrimination based on feedback control of digital ERK responses. *PLoS Biol* 3:e356.
4. Stefanova, I., B. Hemmer, M. Vergelli, R. Martin, W. E. Biddison, and R. N. Germain. 2003. TCR ligand discrimination is enforced by competing ERK positive and SHP-1 negative feedback pathways. *Nat Immunol* 4:248-254.
5. Tian, T., A. Harding, K. Inder, S. Plowman, R. G. Parton, and J. F. Hancock. 2007. Plasma membrane nanoswitches generate high-fidelity Ras signal transduction. *Nat Cell Biol* 9:905-914.
6. Harding, A., and J. F. Hancock. 2008. Ras nanoclusters: combining digital and analog signaling. *Cell Cycle* 7:127-134.
7. Barnden, M. J., J. Allison, W. R. Heath, and F. R. Carbone. 1998. Defective TCR expression in transgenic mice constructed using cDNA-based alpha- and beta-chain genes under the control of heterologous regulatory elements. *Immunol Cell Biol* 76:34-40.
8. Kingeter, L. M., and B. C. Schaefer. 2008. Loss of protein kinase C $\theta$ , Bcl10, or Malt1 selectively impairs proliferation and NF-kappaB activation in the CD4+ T cell subset. *J Immunol* 181:6244-6254.



## **Chapter 4: Discussion**

### ***Review of Chapter 2 results***

As described in Chapter 2, CD4<sup>+</sup> and CD8<sup>+</sup> T cells are differentially affected by the loss of the proteins PKCθ, Bcl10, and Malt1. Specifically, knock-out CD4<sup>+</sup> T cells showed a severe proliferative defect after TCR ligation, while knock-out CD8<sup>+</sup> T cells were less affected, and a sub-population of knock-out CD8<sup>+</sup> T cells proliferated to the same extent as WT CD8<sup>+</sup> T cells (Ch. 2: Fig. 1D). Consistent with previously published results, knock-out T cells showed a defect in IL-2 production following TCR ligation (Ch. 2: Fig. 3A-B). Examination of surface activation marker expression revealed that knock-out CD4<sup>+</sup> and CD8<sup>+</sup> T cells upregulate CD44 and CD25 following TCR ligation (Ch. 2: Fig. 3C-D). The expression of CD25 on the surface of knock-out T cells suggested these cells retain the ability to respond to IL-2; however, the addition of exogenous IL-2 did not restore knock-out CD4<sup>+</sup> proliferation (Ch. 2: Fig. 4). Interestingly, exogenous IL-2 did improve knock-out CD4<sup>+</sup> T cell survival, and had a positive effect on the survival of proliferating knock-out CD8<sup>+</sup> T cells (Ch. 2: Fig. 5). These results suggest that the proliferative and pro-survival effects of IL-2 are mechanistically separable, consistent with

previously published data (1). Examination of NF- $\kappa$ B activation showed that knock-out CD4<sup>+</sup> T cells had a striking defect in NF- $\kappa$ B activation, as evidenced by decreased levels of phospho-I $\kappa$ B $\alpha$  compared to WT CD4<sup>+</sup> T cells (Ch. 2: Fig. 6). In contrast, knock-out CD8<sup>+</sup> T cells showed a less severe defect in NF- $\kappa$ B activation, and reminiscent of the proliferation data, a subset of knock-out CD8<sup>+</sup> T cells achieved the same degree of NF- $\kappa$ B activation as WT CD8<sup>+</sup> T cells. Examination of proliferating knock-out and WT CD8<sup>+</sup> T cells revealed little difference in NF- $\kappa$ B activation, suggesting that knock-out CD8<sup>+</sup> T cells that are capable of proliferating are able to overcome signaling defects related to absence of PKC $\theta$ , Bcl10, or Malt1 (Ch. 2: Fig. 6G-H). Overall, our data indicate that CD4<sup>+</sup> and CD8<sup>+</sup> T cells exhibit differential signaling to NF- $\kappa$ B.

### ***CD4<sup>+</sup> and CD8<sup>+</sup> T cells display differential signaling***

While it is easy to think of T cells as being a homogenous population, it is important to remember that CD4<sup>+</sup> and CD8<sup>+</sup> T cells play very different roles in the adaptive immune response. Therefore, it is not surprising that the two cell types exhibit unique signaling characteristics following TCR ligation. An example of this is JNK (jun kinase) signaling. T cells express 2 forms of JNK: JNK1 and JNK2. Recent reports have demonstrated that JNK1 and JNK2 function differently in CD4<sup>+</sup> and CD8<sup>+</sup> T cells (reviewed in (2)). For

example, JNK2 is not required for CD4<sup>+</sup> production of IL-2, but appears to negatively regulate IL-2 production by CD8<sup>+</sup> T cells, as JNK2<sup>-/-</sup> CD8<sup>+</sup> T cells produced more IL-2 than their WT counterparts. Within CD4<sup>+</sup> T cell effector types, T<sub>H</sub>1 and T<sub>H</sub>2 cells also showed differential use of JNK1 and JNK2, indicating that functionally distinct effector cell types exhibit divergent utilization of this signaling pathway.

Another example of differential signaling is revealed by analysis of the transcriptional profile of CD4<sup>+</sup> and CD8<sup>+</sup> T cells. While a large proportion of identified genes showed similar expression patterns in CD4<sup>+</sup> and CD8<sup>+</sup> T cells, a notable collection of genes showed differential expression in CD4<sup>+</sup> and CD8<sup>+</sup> T cells (3). The results of this study provide circumstantial evidence for differential signaling in CD4<sup>+</sup> and CD8<sup>+</sup> T cells, as unique patterns of gene expression can be viewed as a consequence of exploiting different signaling pathways.

In terms of CD4<sup>+</sup> and CD8<sup>+</sup> development, a recent report indicates that NF-κB plays distinct roles in the development of CD4<sup>+</sup> and CD8<sup>+</sup> T cells (4). Expression of a super-repressor IκB $\alpha$  protein (a phosphorylation site mutant of IκB $\alpha$  that is not proteasomally degraded) prevented NF-κB activation and resulted in a decrease of CD8<sup>+</sup> single positive thymocytes, but did not affect selection of CD4<sup>+</sup> single positive thymocytes.

Furthermore, expression of constitutively active IKK $\beta$  effectively eliminated the population of CD4 $^{+}$  single positive thymocytes, underscoring the different requirements for NF- $\kappa$ B signaling that CD4 $^{+}$  and CD8 $^{+}$  T cells display during development.

Finally, the scientific literature abounds with examples of differential signaling among T cell subsets, particularly T<sub>H</sub>1 and T<sub>H</sub>2 subsets (5, 2, 6, 7, 8). Although these subsets are all CD4 $^{+}$  T cells, they are as functionally different from each other as CD4 $^{+}$  and CD8 $^{+}$  T cells, and provide further evidence of the differential use of signaling pathways in T cells.

As evidenced by the above examples, our data add to a growing list of signaling pathways that are differentially utilized in CD4 $^{+}$  and CD8 $^{+}$  T cells. Taken together, these data help further our understanding of T cell function, and may eventually allow the design of drugs and therapeutic agents that can differentially target CD4 $^{+}$  and CD8 $^{+}$  T cell activity.

### *A parallel pathway?*

Overall, the data in Chapter 2 suggest that CD4 $^{+}$  T cells rely heavily on PKC $\theta$ , Bcl10, and Malt1 to transduce activating signals from the TCR to NF- $\kappa$ B. In contrast, CD8 $^{+}$  T cells are less reliant on these proteins, and retain some functional capacity to activate NF- $\kappa$ B in their absence, especially under conditions of strong TCR stimulation.

These results suggest that CD8<sup>+</sup> T cells may utilize an uncharacterized parallel pathway to transduce activating signals from the TCR to NF-κB, allowing them to bypass the use of PKCθ, Bcl10, and Malt1 when necessary (Fig. 1). It appears that this alternate pathway is used to augment signaling to NF-κB under conditions of very strong stimulation through the TCR, as evidenced by increased knock-out CD8<sup>+</sup> T cell responses under conditions of strong TCR stimulation (Ch. 2: Fig. 1A, Fig. 2, Fig. 3D).

**Figure 1. CD4<sup>+</sup> and CD8<sup>+</sup> T cells show differential reliance on PKCθ, Bcl10, and Malt1.** CD4<sup>+</sup> T cells require PKCθ, Bcl10, and Malt1 to activate NF-κB. In contrast, under conditions of strong stimulation, CD8<sup>+</sup> T cells utilize an unidentified parallel pathway to activate NF-κB, bypassing PKCθ, Bcl10, and Malt1.

It is tempting to speculate that this ‘parallel pathway’ is nothing more than CD28 co-stimulation providing auxiliary signaling to NF-κB in the absence of functional TCR signaling. However, there are several problems with this explanation. First, with the exception of CD28 superagonist antibodies (9), CD28 signaling alone does not result in T cell activation. Secondly, CD28 signaling to NF-κB is known to involve PKCθ (reviewed in (10, 11)), so in PKCθ<sup>-/-</sup> T cells there should be little observable NF-κB activation. Finally, our results demonstrate a relationship between the strength of TCR stimulus and the response of knock-out T cells (Ch. 2: Fig. 1A, Fig. 2, Fig. 3D, Fig. 6A and H). Since the strength of CD28 co-stimulation was kept constant throughout these experiments, we would not expect the T cell response to change with increasing TCR stimulation if co-stimulatory signaling alone was responsible for T cell activation. Therefore, it is likely that

an alternative TCR-mediated NF-κB activation pathway is responsible for the signaling seen in knock-out CD8<sup>+</sup> T cells.

***What are the roles of PKCθ, Bcl10, and Malt1 in TCR signaling to NF-κB?***

While our data provide an example of differential signaling to NF-κB, many questions remain about the individual roles of PKCθ, Bcl10, and Malt1 in this signaling pathway. Of particular interest is the role these proteins play in memory versus naïve T cells. A recent report found that Bcl10 is required for naïve CD4<sup>+</sup> and naïve and memory CD8<sup>+</sup> proliferation and expression of IL-2, but is dispensable for memory CD4<sup>+</sup> T cell proliferation and IL-2 production (12). The authors suggest that NF-κB activation is not required for memory cell function, although given the pro-proliferative and pro-survival effects of NF-κB, it is not clear why memory T cells would not utilize this transcription factor. The authors did not examine the survival of Bcl10<sup>-/-</sup> memory CD4<sup>+</sup> T cells, and it is possible that while these cells can proliferate and produce IL-2, they show impaired survival in the absence of NF-κB signaling. Nevertheless, these results are intriguing, and suggest that a straightforward comparison between naïve and memory knock-out T cell proliferation and NF-κB activation would help determine the role played by PKCθ, Bcl10, and Malt1 during a primary and secondary activation event.

Another unresolved question is if the population of knock-out T cells that do proliferate and activate NF-κB effectively form memory T cells to the same extent as their

WT counterparts. Examination of the number of memory cells in  $Bcl10^{-/-}$  mice revealed a defect in  $CD4^+$  memory cell number compared to WT mice, suggesting that in the absence of  $Bcl10$ , memory cells do not form properly (12). This decrease in memory cell number may be due to a smaller number of naïve T cells undergoing activation and differentiation to memory cells, or it may reflect a requirement for  $Bcl10$  in the generation of a memory T cell. This study did not examine memory T cell differentiation after an infection, and it would be useful to determine if memory  $CD4^+$  and  $CD8^+$  T cells develop following an acute infection in  $PKC\theta^{-/-}$ ,  $Bcl10^{-/-}$ , and  $Malt1^{-/-}$  mice. Memory cell formation depends in part on a successful primary immune response, and it will be necessary to determine to what degree knock-out animals can successfully respond to viral and bacterial pathogens.

A report examining  $PKC\theta^{-/-}$  responses to viral infections (influenza or LCMV) showed that  $PKC\theta$  was not required for the primary or memory *in vivo* response, suggesting that physiological signals (such as TLR activation of dendritic cells) compensate for the loss of  $PKC\theta$  during a  $T_H1$  response (13). Another possibility is that these viral infections resulted in strong signals through the TCR, which our *in vitro* data suggest is sufficient to trigger the response of  $PKC\theta^{-/-} CD8^+$  T cells. While  $PKC\theta^{-/-}$  mice are capable of mounting a successful  $T_H1$  response, an earlier study revealed defective  $T_H2$  responses to parasite infection (14). These data suggest that the loss of  $PKC\theta$  (and possibly  $Bcl10$  and  $Malt1$ ) does not result in a global immunodeficiency, but rather impairs different types of

effector responses.

Another question of interest concerns the activation of NF- $\kappa$ B; specifically, which NF- $\kappa$ B family members are activated in the absence of PKC $\theta$ , Bcl10, and Malt1. A recent study of B cell activation found that Bcl10 was required for RelA and cRel activation and expression of anti-apoptotic proteins, while Malt1 was necessary for cRel activation (15). It would be useful to determine if a similar phenotype is observed in T cells, and if the loss of PKC $\theta$  affects signaling to different NF- $\kappa$ B subunits.

In addition to revealing signaling differences between CD4 $^{+}$  and CD8 $^{+}$  T cells, the data in Chapter 2 provide evidence of distinct degrees of functional impairment among knock-out T cells. PKC $\theta^{-/-}$  T cells are the most functionally affected, as these cells exhibit the least proliferation, minimal upregulation of CD44 and CD25, and smallest amount of I $\kappa$ B $\alpha$  phosphorylation in response to TCR engagement (Ch. 2: Fig. 1B-D, Fig. 3C-D, Fig. 6A and D-F). In contrast, Malt1 $^{-/-}$  T cells showed the least impairment, with CD8 $^{+}$  T cells in particular displaying almost WT levels of proliferation, CD44 and CD25 upregulation, and I $\kappa$ B $\alpha$  phosphorylation following TCR ligation (Ch. 2: Fig. 1, Fig. 3C-D, Fig. 6E-F). The extreme functional defects of PKC $\theta^{-/-}$  T cells are likely due to additional signaling impairments, as these cells also show defective NFAT activation following TCR ligation (16). Interestingly, the almost normal function of Malt1 $^{-/-}$  T cells, and CD8 $^{+}$  T cells in particular, suggests that Malt1 is not absolutely required for NF- $\kappa$ B activation. Malt1 was

shown to be largely dispensable for BCR-mediated activation of NF- $\kappa$ B in B cells (17), but the same study showed a requirement for Malt1 in TCR-mediated activation of NF- $\kappa$ B in T cells. Collectively, these results and the data in Chapter 2 demonstrate that the function of Malt1 in TCR-mediated signaling to NF- $\kappa$ B is not fully understood.

### *Additional future studies*

Although our data indicate knock-out CD8 $^{+}$  T cells may utilize a second pathway to activate NF- $\kappa$ B, the mechanism of this proposed pathway remains unknown. It is possible that previously characterized binding partners such as TRAF6 or caspase-8 can still mediate signaling in the absence of PKC $\theta$ , Bcl10, or Malt1, particularly in response to strong signals through the TCR. To explore this possibility, it will be necessary to more fully characterize the activity of TRAF6 and caspase-8 in knock-out T cells.

A recent report showed that TRAF6 and caspase-8 inducibly associate with Carma1 during TCR signaling (18). Interestingly, TRAF6 association with Carma1 was not significantly impaired in the absence of Bcl10 or Malt1, although caspase-8 association with Carma1 was negatively affected. Furthermore, Carma1 was able to associate with the

IKK complex in the absence of Bcl10 and Malt1, suggesting that in Bcl10 $^{-/-}$  and Malt1 $^{-/-}$  T cells, Carma1 and TRAF6 should still be able to transduce activating signals to the IKK

complex. Our data support this interpretation, as Bcl10 $^{-/-}$  and Malt1 $^{-/-}$  CD8 $^{+}$  T cells retain

some capacity to activate NF- $\kappa$ B (Ch. 2: Fig. 6C, E, F). In contrast, in PKC $\theta$  $^{-/-}$  T cells, Carma1 should not undergo the conformational change required for interaction with

TRAF6 and the IKK complex, resulting in the more severe defects in NF- $\kappa$ B activation seen in PKC $\theta^{-/-}$  T cells. To formally test this hypothesis, a series of co-immunoprecipitation experiments performed with PKC $\theta^{-/-}$  and WT cells could be used to determine TRAF6 and Carma1 interactions in the absence of PKC $\theta$ . In addition, it would be useful to compare TRAF6 and Carma1 interactions in CD4 $^{+}$  and CD8 $^{+}$  T cells, as variabilities may contribute to differential signaling to NF- $\kappa$ B.

With regard to caspase-8 function, preliminary data indicates that caspase-8 activity is not impaired in knock-out T cells, suggesting that caspase-8 activation is not controlled by PKC $\theta$ , Bcl10, or Malt1. Therefore, it is feasible that caspase-8 contributes to knock-out T cell function. To explore this possibility, caspase-8 could be pharmacologically inhibited and CD8 $^{+}$  proliferation and NF- $\kappa$ B activation examined following TCR ligation. Since caspase-8 $^{-/-}$  mice are unable to mount successful anti-viral responses *in vivo* (19), it is likely that inhibition of caspase-8 function will reduce or eliminate knock-out CD8 $^{+}$  T cell responses following TCR ligation.

Finally, the potential for differential utilization of NF- $\kappa$ B subunits in knock-out T cells suggests that knock-out T cells may exhibit a different pattern of gene expression following TCR ligation, compared to WT cells. A microarray could be used to compare gene expression in WT versus knock-out CD8 $^{+}$  T cells following TCR ligation, to determine what differences in gene expression are found between the two cell types.

Identifying differences in gene expression between WT and knock-out T cells would help to further characterize the activation of knock-out T cells, and furthermore provide information regarding the role of PKC $\theta$ , Bcl10, and Malt1 in the regulation of gene expression during T cell activation.

In summary, our data provide unexpected information regarding the function of PKC $\theta$ , Bcl10, and Malt1 in TCR signaling to NF- $\kappa$ B. These data reveal that the loss of these proteins has unique and quantifiable effects on T cell function, and challenges some of the assumptions made about the individual roles of PKC $\theta$ , Bcl10, and Malt1 in T cell biology. Furthermore, these results provide one of the first examples of differential NF- $\kappa$ B signaling in mature CD4 $^{+}$  and CD8 $^{+}$  T cells, forcing us to re-examine our understanding of how T cells signal to this important transcription factor.

### ***Review of Chapter 3 results***

As described in Chapter 3, the terminal events in TCR-mediated activation of NF- $\kappa$ B, specifically phosphorylation of I $\kappa$ B $\alpha$  and p65, are digital. In response to stimulation with low concentrations of anti-TCR $\beta$ , T cells showed little to no phosphorylation of I $\kappa$ B $\alpha$  (Ch. 3: Fig. 1A). However, stimulation with moderate or high concentrations of anti-TCR $\beta$  resulted in the appearance of an activation peak corresponding to phospho-I $\kappa$ B $\alpha$ . The intensity of this activation peak was relatively stable across anti-TCR $\beta$  concentrations (Ch. 3: Fig. 1B), indicating that once the threshold for signaling had been met, the intensity of the output signal (phospho-I $\kappa$ B $\alpha$ ) was not affected by the intensity of the input signal (anti-TCR $\beta$  concentration). There was a positive correlation between anti-TCR $\beta$